REVIEW

Recent advances in oxidative phenol coupling for the total synthesis of natural products

Matthew C. Carson[a] and Marisa C. Kozlowski[a]*

Received 22nd February 2023,
Accepted 00th January 20xx

DOI: 10.1039/x0xx00000x

Covering: 2008 to 2023

Focusing on advances from the last decade, this review will describe oxidative phenol coupling as applied in the total synthesis of natural products. This review covers catalytic and electrochemical methods with a brief comparison to stoichiometric and enzymatic systems assessing their practicality, atom economy, and other measures. Natural products forged by C–C and C–O oxidative phenol couplings as well as from alkenyl phenol couplings will be addressed. Additionally, exploration into catalytic oxidative coupling of phenols and other related species (carbazoles, indoles, aryl ethers, etc.) will be surveyed. Future directions of this particular area of research will also be assessed.

1. Introduction

The field of natural product chemistry has been significantly impacted by the emergence of oxidative coupling in the early 20th century.[1, 2] Discovering new ways to couple aryl fragments continues to aid organic chemists in their journey to construct the most intricate molecules found in nature. Phenols and phenolic-type compounds are a common feature seen in natural products. These moieties offer unique redox chemistry which provides access to further derivatization (cyclization, dearomatization, etc.).[3-5] A plethora of biosynthetic pathways involve phenol reactivity, especially oxidative coupling of these species.[6-9] As a result, developing oxidative phenolic coupling methods has remained an important challenge in organic chemistry.[10, 11] **Fig. 1** illustrates the citation and publication count from 1961 to present day on oxidative phenol coupling.

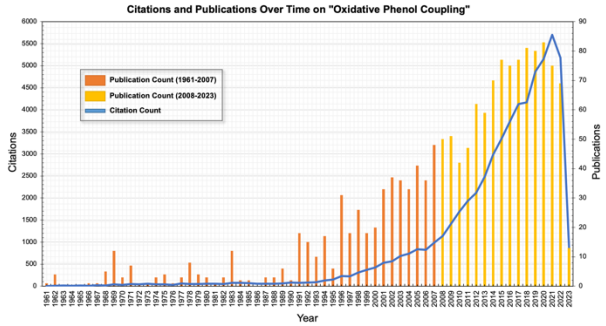

Fig. 1 Graph of publications/citations on "oxidative phenol coupling" from 1961 to 2023 from a Web of Science topic search. (Citation Report graphic is derived from Clarivate *Web of Science*, Copyright Clarivate 2023. All rights reserved.)

This review highlights recent synthetic uses of catalytic and electrochemical oxidative phenol couplings in the total synthesis of natural products with an additional motivation in providing a general outlook for the future. Stoichiometric and enzymatic syntheses are canvassed as a means of comparison to catalytic routes. Key factors and general considerations in oxidative coupling are discussed. The natural products are divided based on their respective chemo- and regioselectivity. The natural products to be discussed are shown in **Fig. 2**.

[a] *Department of Chemistry, Roy and Diana Vagelos Laboratories, University of Pennsylvania, Philadelphia, Pennsylvania 19104-6323, United States*

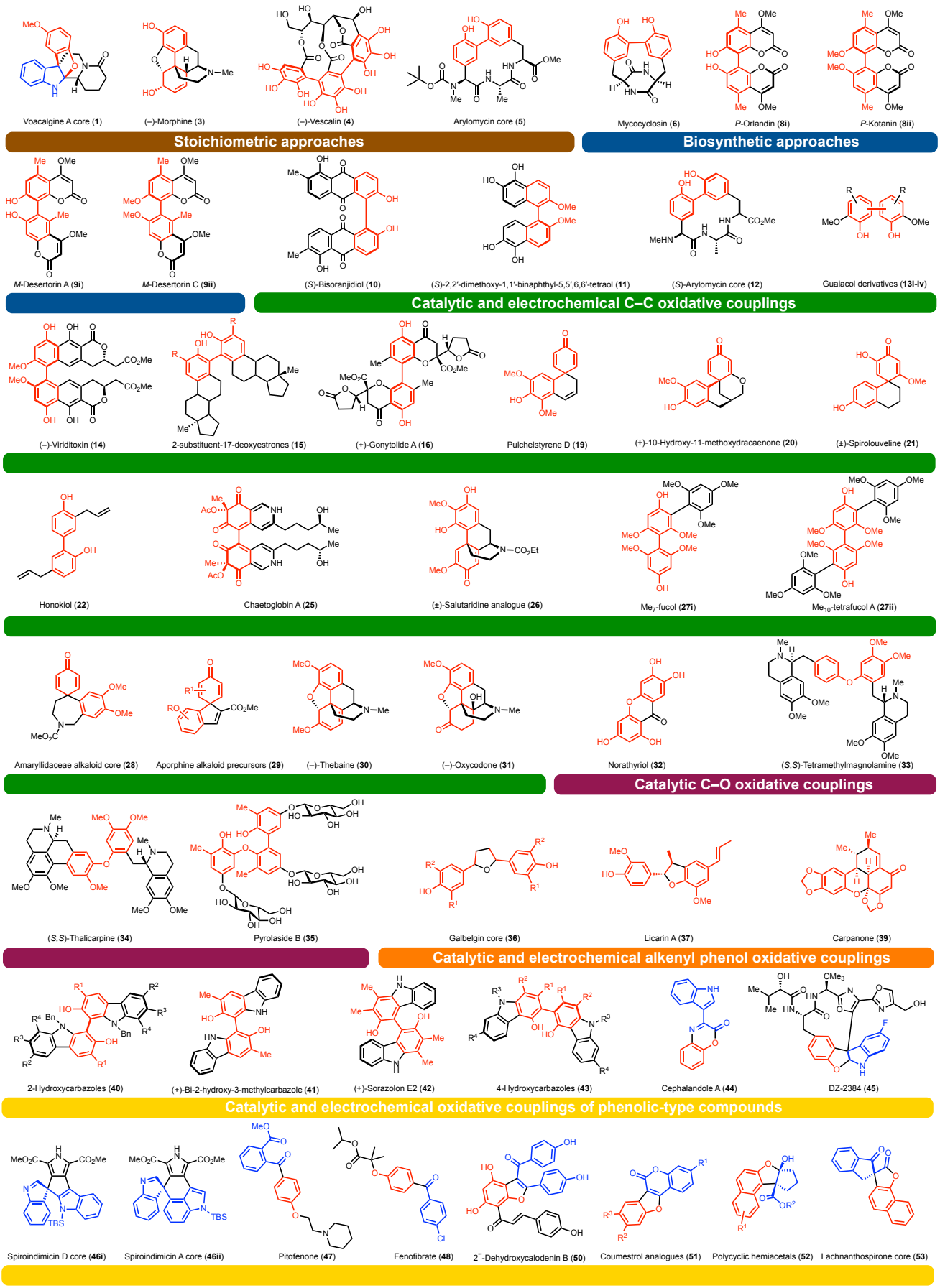

Fig. 2 Representative natural products forged by oxidative phenolic couplings categorized by approach used.

2. Fundamentals of oxidative phenol coupling

Oxidative coupling serves as a powerful synthetic technique in constructing new phenolic connections. It offers good functional group tolerance and operates under mild reaction conditions as phenol oxidation is facile. In comparison to other cross-coupling methods, no prefunctionalization (aryl bromides, boronic acids, etc.) is required as the inherent reactivity of each ring is utilized. However, controlling multiple reactive sites remains a challenge and can lead to undesired coupling products. Recent advances in the field have improved upon these selectivity issues by biasing the substrate and developing catalyst features, those of which will be later discussed.

Various products from a general phenol oxidation are illustrated in **Scheme 1**. If multiple sites are available for reaction, coupling at the *para* position tends to dominate. One gambit to predispose a substrate for *ortho* coupling is the installation of blocking substituents at the *para* position. Pummerer ketone products, such as usnic acid, arise from an important subclass of phenol couplings that involve an additional intramolecular cyclization.[12-14] When these coupling products were first introduced in the literature in 1925 by Pummerer *et al.,* the authors postulated that the reaction proceeded via a C-O coupling at the *para* position of *p*-cresol followed by a radical cyclization.[15] Dismayed by the lack of mechanistic evidence provided in the prior work, Barton *et al.* published a full follow-up paper refuting the mechanism and structure of the Pummerer ketone.[14, 16] The authors argued that the post-coupling radical intermediate proposed by Pummerer *et al.* would not undergo cyclization, but rather oxidation to a *para*-phenoxy quinone. Rather, Barton *et al.* proposed that a C-C *ortho-para* coupling of *p*-cresol would afford a neutral quinone intermediate that would undergo β-addition of the hydroxyl to the quinone to furnish the Pummerer ketone. Their revised mechanism and structure remains accepted in the literature today. However, Pummerer ketone products will not be discussed here as there are no recent advances.

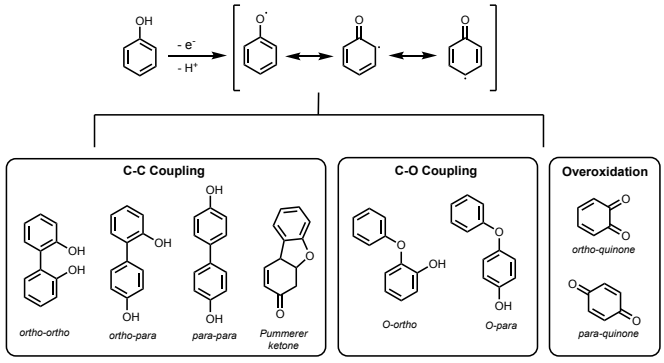

Scheme 1 Potential products from one-electron/proton transfer of phenol.

Sir Derek Barton was one of the early pioneers of oxidative phenol couplings in the 1950s, establishing many of the precedents in which modern applications rely upon. A 1957 perspective from Barton *et al.* intricately details the various phenol coupling mechanisms at the time and their biosynthetic application in the synthesis of alkaloids, fungal metabolites, and other plant-derived natural products.[17] Kozlowski and co-workers recently disclosed a perspective on oxidative phenol coupling methods[18], while the current review focuses on applications to natural product synthesis. Oxidative coupling and its role in asymmetric biaryl formation for natural product synthesis is also outlined in a review by Kozlowski *et al.*, which serves as a main repository for pre-2008 work.[19] Several research groups have conducted thoughtful analyses of the chemo- and regio-selectivity of oxidative phenol coupling for iron[20-22], chromium[23, 24], copper[25, 26], and vanadium[27, 28] systems. In these works, oxidation potentials, global/site nucleophilicities, Sterimol values, and pK_a values are utilized to gain control of homo- versus heterocoupling of phenols and other related structures. In one report, the authors discuss how over-oxidation is a common issue as dimeric products are often more oxidizable than their monomeric forms so various oligomeric products can be obtained.[29] Takizawa and co-workers have presented a perspective on the use of vanadium catalysts in the atroposelective synthesis of axially chiral compounds via oxidative coupling.[30]

Oxidative coupling of phenols can be accomplished through chemical, electrochemical, photochemical, and biosynthetic approaches. The groups of Kozlowski[23, 24], Pappo[20-22], and Lumb[25, 31] have established several precedents for these chemical transformations utilizing metal catalysts and molecular oxygen or peroxides as terminal oxidants. The field of electrochemical oxidative couplings have been pioneered by Waldvogel[32-36] and Opatz[35-37]. By utilizing biosynthetic pathways, the Narayan[38-41] and Müller[42-44] groups have developed enzymatic approaches to tackle these couplings. Photochemistry has also recently emerged as a useful technique to achieve phenolic transformations including dearomatizations and oxidative couplings.[29, 45-48]

3. Stoichiometric approaches

An abundance of stoichiometric oxidative couplings have been reported in the synthesis of biologically active compounds. The use of stoichiometric oxidants and metals raises concerns over functional group tolerance as well as scalability. Typical procedures utilize stoichiometric loadings of first-row transition metal reagents or hypervalent iodine complexes. Using these approaches, many research groups have succeeded in synthesizing natural products via key oxidative coupling steps. Selected examples of intermolecular couplings by the Vincent group are outlined in **Scheme 2**. In the first case, one substrate undergoes a discrete oxidation to an iodinated intermediate generating an electrophile *in situ* that then reacts with the second nucleophilic partner (**Scheme 2a**). Specifically, **1b** reacts with stoichiometric oxidant NIS to generate an intermediate that can engage phenol **1a** in a Friedel-Crafts reaction and cyclization to furnish the voacalgine A core (**1**) in 26% yield.[49]

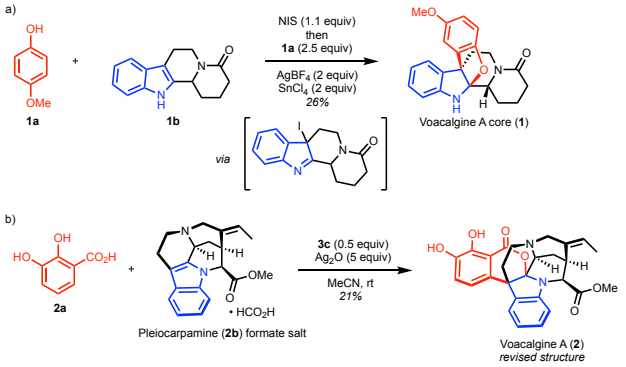

Scheme 2 Stoichiometric couplings of phenols and indoles.

However, further synthetic endeavors by Vincent and co-workers discovered that their originally assigned framework was incorrect. A stoichiometric Ag_2O coupling of phenol **2a** and pleoiocarpamine (**2b**) formate salt afforded the revised structure of voacalgine A (**2**) in 21% yield (**Scheme 2b**).[50] This method proceeds via an *ortho*-quinone intermediate which undergoes 1,4-addition with the indole. Subsequent trapping of the resultant iminium by the carboxylate then provides voacalgine A (**2**). The dimeric natural product bipleiophylline (not shown) was also formed albeit in very low yield of 3%. The authors use 2D-NMR analysis to support the assignment of this isochromenoindoline skeleton. Notably, the yields in these stoichiometric processes are not high, highlighting the difficulty in performing these complex oxidative couplings. The products of oxidative phenol couplings are prone to overoxidation as they can often be more oxidizable than the starting materials. Employing harsh oxidative conditions can therefore further degrade potential product formation.[18, 51]

Intramolecular versions of oxidative couplings have also been employed in total synthesis. In 2014, the Gaunt group reported an enantioselective formal synthesis of (–)-morphine (**3**).[52] An *ortho-para* oxidative phenol coupling provided a key early-stage intermediate on a multigram scale (**Scheme 3**). This intramolecular oxidative coupling of **3a** was accomplished with $PhI(OAc)_2$ to form the biaryl bond (highlighted in green) and DBU-promoted desymmetrization aided in the production of intermediate **3b** with 48% yield over two steps (10 gram scale) resulting in a formal synthesis of (–)-morphine (**3**). Literature precedent exists for the completion of (–)-morphine (**3**) from **3b** in 16 additional steps.[53, 54]

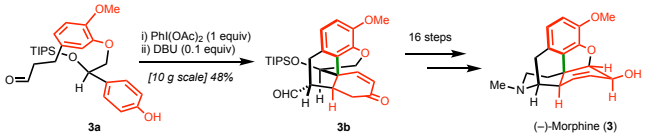

Scheme 3 Stoichiometric *ortho-para* coupling in formal synthesis of morphine.

Often, late-stage intramolecular oxidative couplings are employed in total synthesis, typically through biomimetic routes. (–)-Vescalin (**4**), a unique polyphenolic natural product, was synthesized utilizing a sequence of oxidative couplings as shown in **Scheme 4**.[55] The C1-C2 connection in **4a** was first assembled with a $CuCl_2$-*n*$BuNH_2$ oxidative system in a 58% yield with 5 and 20 equivalences, respectively. In this process only the (*S*)-atropisomer was obtained. The core of (–)-vescalin (**4**) was furnished with a final atroposelective oxidative coupling to connect C3-C4 in 41% yield with $CuCl_2$ (5 equiv) and bispidine (20 equiv). Hydrogenation and acidic workup completed the sequence to (–)-vescalin (**4**) which was comprised of 16 steps with an overall yield of around 2%. Yamada and co-workers also disclosed an atroposelective $CuCl_2$-*n*$BuNH_2$ method which was used in the total synthesis of (–)-strictinin (not shown), a gallate-derived natural product, in a related intramolecular coupling.[56] The axial chirality of the hexahydroxydiphenoyl (HHDP) moieties found in compounds like (–)-vescalin (**4**) was recently elucidated by Wakamori and co-workers. Notably, the (*S*)-atropisomer formed initially and then isomerized to the natural (*R*)-configuration.[57]

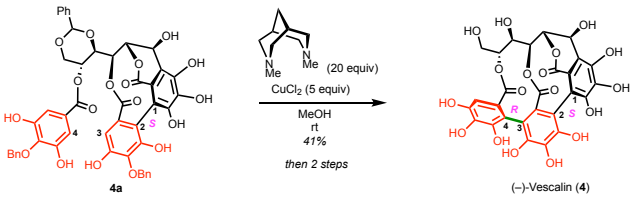

Scheme 4 Biomimetic total synthesis of (–)-vescalin.

The Baran group accessed the arylomycin core (**5**) with an oxidative phenol coupling via a Cu(III)-TMEDA system (**Scheme 5**).[58] Their approach involved a biomimetic *ortho-ortho* intramolecular cyclization of **5a** to form the arylomycin core (**5**) in 51–70% yields. The method scaled well with a five gram scale reaction proceeding in 60% yield. Molecular oxygen proved to be the optimal terminal oxidant in this chemistry as stronger oxidants such as oxone and H_2O_2 led to lower yields. With access to the core via this early-stage approach, the authors concisely synthesized an array of derivatives which allowed for the study of their antibacterial properties.

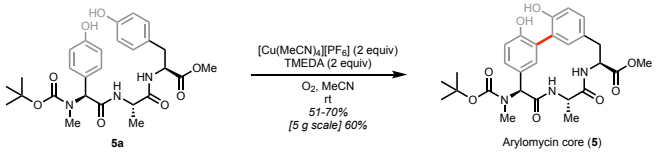

Scheme 5 Baran's stoichiometric synthesis of arylomycin core.

4. Enzymatic approaches

Oxidative biaryl bond formation is ubiquitous across many classes of natural products and synthetic chemists have made tremendous strides in completing these transformations using innovative chemical approaches. However, the unique environments provided by enzymes in biological systems have proven difficult to replicate for these processes. These selective biocatalytic transformations offer impressive functional group tolerance and overall efficiency. Within the last two decades, directed evolution has allowed for the optimization of different enzymes such that these transformations can be performed on non-natural substrates with efficiencies approaching or rivaling those of conventional organic reactions. Enzymes such as horseradish peroxidase (HRP) have found utility in oxidative

phenol coupling in the presence of sensitive functional groups.[59, 60] Müller and co-workers have summarized many of the enzymatic approaches towards intermolecular phenol oxidative coupling.[44] Cytochrome P450 enzymes have proven to be useful platforms as shown elegantly by the Narayan group.[41]

As previously demonstrated, arylomycins are an important class of antibiotic compounds with phenolic biaryl backbones and present a considerable synthetic challenge. Prior to the stoichiometric oxidative coupling of the arylomycin core (**5**) by Baran and co-workers (see **Scheme 5** above), Dorrestein *et al.* discovered the gene cluster responsible for production of the arylomycins in *Streptomyces roseosporus*.[61] This work paved way for chemists to bioengineer these clusters to make different arylomycin analogues. In a recent report, an engineered cytochrome P450 enzyme was utilized to accomplish the oxidative cyclization of two phenol units (*ortho-ortho*) to form the arylomycin core (**5**) on gram-scale in 84% assay yield.[62]

Intramolecular oxidative couplings are difficult to achieve chemically, especially for strained ring systems, but enzymes can facilely accomplish these reactions. Mycocyclosin (**6**), a diketopiperazine metabolite isolated from *Mycobacterium tuberculosis*, contains a highly strained dityrosine framework. Martí and co-workers used the gene rv2276 which encodes for a P450 enzyme, CYP121, for the oxidative C–C bond formation of **6a** to form mycocyclosin (**6**) (**Scheme 6**).[63] This enzyme is found exclusively in *M. tuberculosis* and this is its only known biocatalytic activity. Work by the Hutton[64] and Schindler[65] groups have leveraged Pd(II)-catalyzed Suzuki-Miyaura and Ullman-type couplings in their respective total syntheses of mycocyclosin (**6**), but no catalytic oxidative coupling methods have been successful.

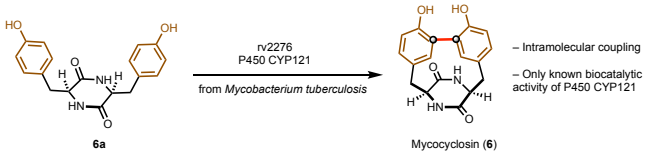

Scheme 6 Biogenetic oxidative coupling of mycocyclosin.

There has been lots of work on enzymatic intramolecular oxidative couplings, but biomolecular intermolecular couplings are much less common. The Müller group developed cytochrome P450 enzymes for the stereo- and regioselective synthesis of axially chiral phenolic natural products.[43] Using P450 enzymes KtnC and DesC (expressed in *Saccharomyces cerevisiae* fungi*)*, the authors were able to synthesize *P*-orlandin (**8i**) and *M*-desertorin A (**9i**), respectively, from the same starting material **7** (**Scheme 7**). This divergent approach highlights the regio- and stereoselectivity of P450 enzymes in fungi. Additionally, there are literature precedents for the synthesis of *P*-kotanin (**8ii**) from *P*-orlandin (**8i**).[66] While the synthesis of *M*-desertorin A (**9i**) to *M*-desertorin C (**9ii**) has not been reported, it should also be feasible. Recently, the fungal P450 KtnC was also expressed in yeast to accomplish the *in vivo* biosynthesis of *P*-orlandin (**8i**) by Narayan and co-workers.[67]

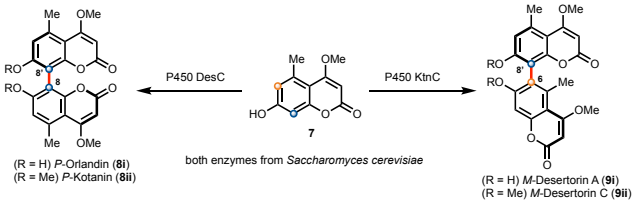

Scheme 7 Regioselective biocatalytic synthesis of *p*-orlandin and *m*-desertorin A.

5. Catalytic and electrochemical C–C oxidative couplings

The formation of C–C bonds via oxidative coupling methods are an especially useful transformation. Without the need for prefunctionalization, new connections between aryl fragments can be forged in fewer synthetic manipulations. Catalytic and electrochemical methods for these reactions allow for more efficient processes that minimize waste and improve upon atom economy while maintaining synthetic efficacy. Within C–C oxidative phenol coupling, a variety of regioselective outcomes can be observed as previously described in **Scheme 1**. The following section will discuss these transformations based on the different coupling patterns (*ortho-ortho*, *para-para*, *ortho-para*, and others).

5.1 *ortho-ortho* couplings

Axially chiral phenolic natural products have been common targets amongst those working in the oxidative coupling community. In 2012, the Kozlowski group disclosed an asymmetric naphthol oxidative coupling with a catalytic Cu-cyclic amine system in the total synthesis of (*S*)-bisoranjidiol (**10**).[68] With molecular oxygen as the oxidant, this approach allowed for the homocoupling of **10a** to afford (*S*)-**10b** in 62% yield and 87% ee (**Scheme 8**). An additional nine synthetic steps led to the completion of (*S*)-bisoranjidiol (**10**). Attempts to couple the anthracene or anthraquinone units (biomimetic approaches) failed with the former oxidizing to the corresponding anthraquinones and the latter proving resistant to oxidation. As such, the authors coupled the naphthol fragments and then constructed the remaining ring of the anthraquinone via Diels-Alder reactions. In a follow-up publication, divergent syntheses of this framework were achieved to furnish bisanthraquinone analogues (not shown).[69]

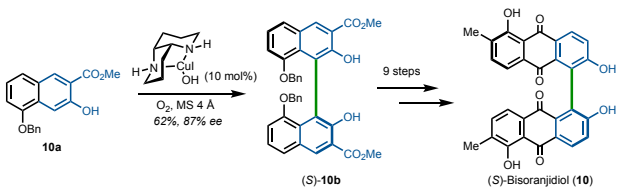

Scheme 8 Oxidative coupling in the total synthesis of (*S*)-bisoranjidiol.

In 2007, a research group from the University of Mississippi isolated a marine natural product from the Indonesian sponge *Lendenfeldia sp.* and determined its structure to be (*S*)-**11** via NMR analysis.[70] The Kozlowski group set out in 2012 to synthesize this natural product via an asymmetric oxidative

coupling.[71] From naphthol **11a,** a chiral dimeric vanadium catalyst gave rise to (*S*)-**11b** in 82% yield and 81% ee which was confirmed by spectroscopy and crystallography (**Scheme 9**). An additional four steps led to the synthesis of (*S*)-**11** in 70% yield. When the authors compared their spectra and physical properties (solubility, air/silica stability, etc.) with those reported from the isolation, they discovered that they did not match. With further analysis, Kozlowski and co-workers determined that the isolated material from the plant was actually a tetrabrominated diphenyl ether compound.

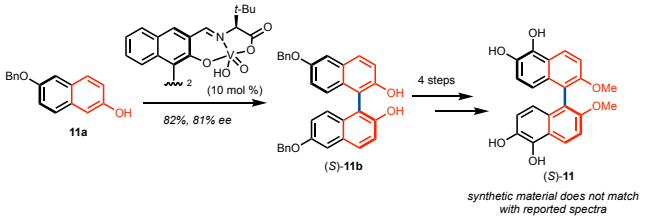

Scheme 9 Atroposelective oxidative coupling in marine metabolite structural revision.

Pappo and co-workers implemented an intermolecular catalytic oxidative cross-coupling method to assemble the arylomycin core and analogues thereof.[72] As discussed before, the intramolecular cyclizations proved difficult. In addition, direct oxidative coupling of tyrosine derivatives is challenging due to over oxidation to trimers, etc.[9] As such, substrates **12a** and **12b** with *tert*-butyl groups, which both blocked formation of higher order adducts and improved reactivity, were employed. Intermolecular cross-coupling using an iron porphyrin catalyst produced **12c** in 48% yield (**Scheme 10**). To obtain optimal yields, the slow addition of the oxidant (*m*-CPBA) and **12b** in small portions was needed. Protecting group removal/macrolactamization and *tert*-butyl cleavage afforded the (*S*)-arylomycin core (**12**) in 60% yield over three steps. Pappo and co-workers were also able to access the core of polycyclic peptide RP 66453 (not shown).

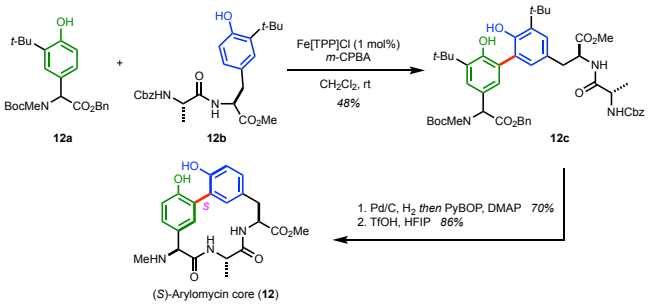

Scheme 10 Intermolecular catalytic cross-coupling approach to arylomycin core.

Oligomers of guaiacol, a phenolic natural product, are commonly found in the degradation of lignin and other biosynthetic pathways.[73, 74] These materials also have potential as sustainable aromatic feedstocks. The Waldvogel group applied boron-doped diamond (BDD) anodes in the anodic coupling of guaiacol and analogues as an entry to unsymmetrical bisphenol products.[33] **Scheme 11** highlights an interesting shift in observed regioselectivity by varying the R group at the *para* position of **13a**. The *ortho-meta* product **13i** is obtained in a 33% yield when 4-methyl **13a** is used and *ortho-ortho* **13iv** is formed in a 18% yield with 4-*tert*-butyl **13a**. The isopropyl variant of **13a** led to equal quantities of the *ortho-ortho* (**13ii**) and *ortho-meta* (**13iii**). As the steric bulk increases, the product distribution shifts to favor *ortho-ortho* versus *ortho-meta* homocoupling. It is appears that both the hydroxy and methoxy groups can activate different positions for oxidation and the overall reactivity is dictated by steric effects. The even lower conversion for the isopropyl variant was attributed to its propensity to undergo alternate oxidation reactions including at the benzylic position.

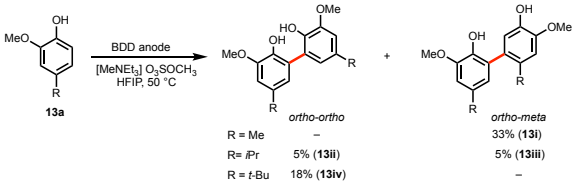

Scheme 11 Regioselectivity in electrochemical oxidative coupling of guaiacol derivatives.

(–)-Viriditoxin (**14**), a fungal natural product with antibacterial properties isolated from *Aspergillus viridinutans*, contains an atropoisomeric biaryl backbone.[75] In 2011, the Shaw group reported the total synthesis of (–)-viriditoxin (**14**) via an asymmetric oxidative naphthol coupling (**Scheme 12a**).[76] At first glance, the backbone appears to be constructed via a *para-para* connection, but it is actually achieved via an *ortho-ortho* coupling with post-functionalization to adjust the phenol alkylation states. The authors accessed **14a** in an eight step sequence, although yields were variable and scale-up was difficult. They then screened a variety of vanadium catalysts to optimize the diastereoselective homocoupling. With $VO(acac)_2$, a 67% yield of **14b** was achieved with moderate diastereoselectivity (76:24 dr). A dimeric (*S,R*)-vanadium catalyst led to the best results with 87% yield and 89:11 dr and led to (–)-viriditoxin (**14**) after five additional synthetic steps. Use of a (*S,S*)-vanadium dimeric catalyst (**Scheme 12b**) in oxidative coupling of analog **14c** resulted in a superior diastereoselectivity (>95:5) albeit with slightly lower yield (85%).[77] An additional synthetic step was required to synthesize (–)-viriditoxin (**14**) in comparison to the former synthesis, but the oxidative coupling precursor **14c** was easier to synthesize on scale. **Scheme 12c** illustrates the proposed asymmetric induction in the coupling process which is governed by the configuration of the pyranone ring and the chiral vanadium catalyst. The diastereomeric transition state **B** is favored as the equatorial configuration of the R group minimizes steric interactions in comparison to the axial hydrogen clash in transition state **A**.

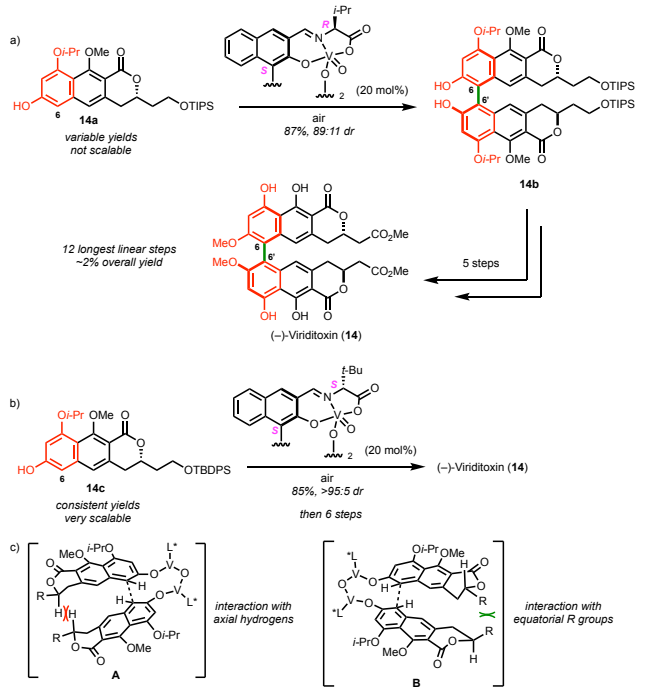

Scheme 12 Oxidative couplings in the total syntheses of (–)-viriditoxin.

An abundance of steroidal compounds contain phenolic frameworks, but their competence in oxidative coupling is not well studied. In 2013, Yu and co-workers disclosed an oxidative coupling of deoxyestrone derivatives with a catalytic copper system.[78] Using $CuCl_2$/TMEDA as a catalyst and air as the terminal oxidant, the authors coupled (*S*)-**15a** to synthesize a variety of 2-substituted deoxyestrone dimers (*S,S*)-**15** in 22–75% yields and 1:1 dr (**Scheme 13**). In order to avoid regioselectivity issues, the authors blocked the 2-position of (*S*)-**15a**. The success of the reaction was highly affected by the steric and electronic nature of the 2-substituent. Large substituents (*tert*-butyl, naphthalene) and electron-rich aryls led to lower yields or even no reactivity.

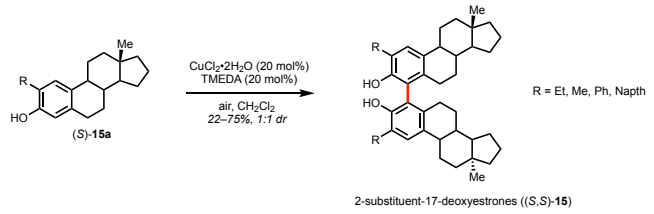

Scheme 13 Oxidative homocoupling of deoxyestrone derivatives.

5.2 *para-para* couplings

Couplings at the *para-para* positions have been reported in a number of systems. However, reaction selectivity remains a complicating factor when both *ortho* and *para* sites are available. One common tactic to address regioselection in this context is to employ blocking groups. The Porco group utilized this strategy in oxidative couplings to generate a dimeric lactone natural product (**Scheme 14**).[79] Specifically, a bromine was strategically installed at the *ortho* position of (±)-gonytolide C generating (+)-**16a** via a kinetic resolution. An asymmetric conjugate reduction strategy using $Cu(OAc)_2$ and Josiphos SL-J001-2 achieved the kinetic resolution (97:3 er post-recrystallization with 49% yield), which yielded (+)-**16a** after bromination. Subsequent oxidative coupling with VOF_3/TFA/TFAA yielded (+)-gonytolide A (**16**) in a 12% yield after dehalogenation. Its unnatural atropisomer, (–)-*atrop*-gonytolide A (not shown), was also obtained in a 35% yield. The bromo group both stabilized radical cation intermediates and aided in the diastereoselectivity of the coupling. The need for such blocking groups to control regioselectivity in oxidative couplings highlights a limitation of current small molecule reagents and catalysts.

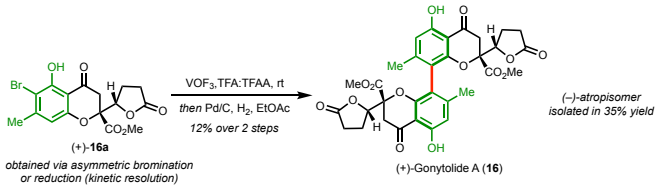

Scheme 14 Atroposelective oxidative coupling in synthesis of (+)-gonytolide A.

In 2011, the Waldvogel group presented a electrochemical *para-para* coupling of guaiacol derivatives which did not require such a blocking approach in order to achieve a selective *para-para* coupling.[33] Using their BDD anodic approach, **17a** was coupled selectively to form the *para-para* dimer **17** in an 83% yield (**Scheme 15**). Methoxy substituents have a tendency to promote *ortho*-quinone formation, so the lack of overoxidation products was surprising to the authors. The oxidation of phenols with BDD anodes offers unique regioselective outcomes, typically unattainable by traditional methods that utilize the steric and electronic bias of the substituents. In addition, the use of 1,1,1,3,3,3-hexfluoro-2-propanol (HFIP) solvent was key and has seen continued use in in both chemical, photochemical, and electrochemical oxidative couplings. Its high polarity and intricate hydrogen-bonding network with aggregating fluorine atoms that creates a unique "solvate cage" stabilizes radical intermediates.[80]

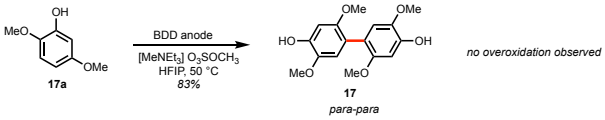

Scheme 15 Electrochemical *para-para* coupling of a guaiacol derivative.

The Pappo group disclosed an oxidative phenol coupling toward the synthesis of fucol-derived natural products in which a blocking group was not employed.[81] Oxidative coupling of **18a** using their $FeCl_3$/*t*-BuOO*t*-Bu system formed *para-para* product *sym*-Me_4-difucol (**18i**) along with *ortho-para unsym*-Me_4-difucol (**18ii**) in 33% and 22% yields, respectively (**Scheme 16**). With both *ortho* and *para* sites open, the method suffered from poor regioselectivity with only a slight preference for *para-para* over *ortho-para* (1.5:1). This outcome highlights the need in the field for development of more selective couplings in the presence of multiple reactive sites.

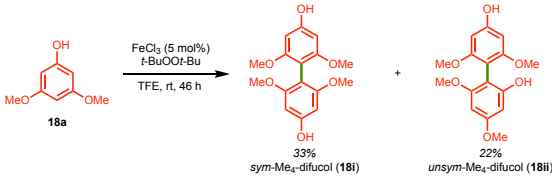

Scheme 16 Iron-catalyzed *para-para* and *ortho-para* oxidative coupling of fucol natural products.

Intermolecular oxidative couplings have been well investigated, but intramolecular approaches have been much more elusive. The Kozlowski lab reported an efficient and mild method for furnishing spirohexadienones via vanadium-catalyzed intramolecular *para-para* oxidative coupling of phenols.[82] Typically, this transformation has been performed with stoichiometric oxidants ($VOCl_3$)[83, 84] or via oxidation of the aryl ether products[85, 86], which follows a different mechanism. Despite there being multiple sites for potential functionalization, only the *para-para* coupled product was seen in optimization of this reaction. This bond formation creates a quaternary carbon center arising from dearomatization of the *para* phenol.

With this method, Kozlowski and co-workers completed the first total synthesis of pulchelstyrene D (**19**). The key step was intramolecular coupling of **19a** with vanadium catalyst **V2** in the presence of O_2 to afford **19b** in 82% yield (**Scheme 17a**). Three additional steps (34% overall) were needed to introduce the alkene backbone which was not tolerated during the oxidative cyclization. The spirocyclic dracaenone natural product, (±)-10-hydroxy-11-methoxydracaenone (**20**), was synthesized in a 78% yield from **20a** using **V2** and molecular oxygen as terminal oxidant (**Scheme 17b**). This compound has been synthesized previously with protected aryl ether approaches[87, 88], but this new method eliminates the need for protecting groups. **Scheme 17c** describes the oxidative coupling of **21a** with a **V2**/O_2 system to produce **21b** in an 88% yield. Subsequent selective deprotection of the isopropyl ether in the presence of the methyl ether led to the formation of (±)-spirolouveline (**21**).

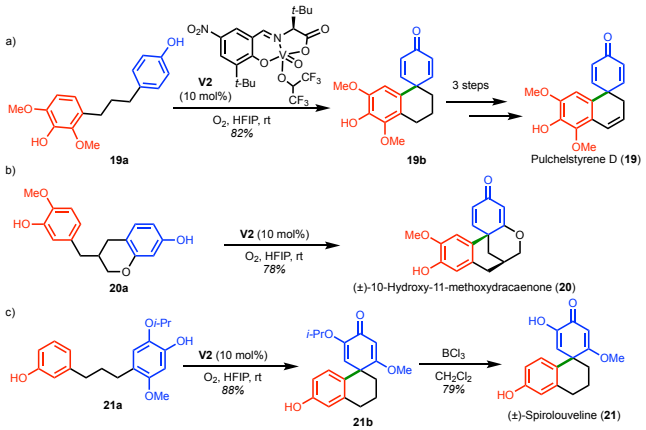

Scheme 17 Intramolecular oxidative coupling to form phenol-dienones.

5.3 *ortho-para* couplings

The bark of magnolia trees, specifically *Magnolia grandiflora*, has a long history for its use in Chinese herbal medicine with anti-inflammatory, anti-oxidant, and a plethora of other desirable biological properties. Honokiol (**22**), a phenolic natural product, was identified as a major active component of these extracts.[89-91] Recently, honokiol (**22**) has found use in potential treatments for cancer and heart disease as well as commercial products like toothpaste. In 2017, the Kozlowski group reported several efficient methods for the total synthesis of honokiol (**22**) utilizing an *ortho-para* oxidative coupling early in the synthesis.[92] **Scheme 18** illustrates one of the approaches in which **22a** and **22b** are cross-coupled with commercially available Cr-Salen-Cy and then de-*tert*-buylated to form **22c** in 85% yield. Five subsequent steps led to the total synthesis of honokiol (**22**). Again, the *tert*-butyl groups serve to block potential reactive positions to limit the regioisomeric outcomes. Overall, this route minimized the use of toxic reagents and long reaction times while providing a lower step count and higher yields.[93-95] Building off of this work, Kozlowski and co-workers also utilized Cr-Salen catalysts to synthesize honokiol-type derivatives leading to analogs that are far more potent against commensal oral bacteria.[91, 96]

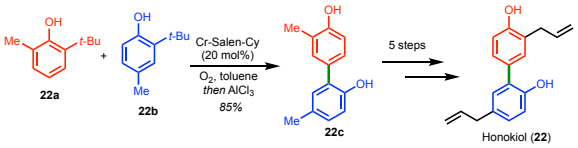

Scheme 18 Oxidative coupling as first step in improved synthesis of honokiol.

5.4 Other C–C couplings of phenols

Some approaches in the literature have accessed unique regioselective products using oxidative coupling or contain highly-oxygenated species in which one specific regioselective outcome cannot be assigned. Continuing with the work of Waldvogel on the coupling of guaiacol derivatives with BDD anodes, the authors were able to assemble some notable regioisomers.[33] **Scheme 19a** shows the coupling of **23a** to form *meta-meta* product **23** in a 45% yield as well as the oxidative coupling of syringol (**24a**) to access a *meta-para* dimer **24** in a 44% yield (**Scheme 19b**). In these cases, the directing effects of the methoxy groups likely compete with those of the hydroxy groups.

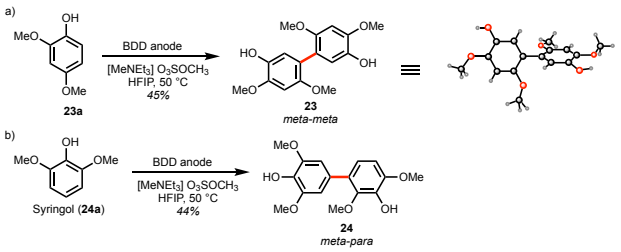

Scheme 19 *meta-meta* and *meta-para* electrochemical oxidative couplings.

Polyketide natural products are abundant across fungal and plant species and possess a wealth of biological activities. A oxygenated axially chiral polyketide, chaetoglobin A (**25**), was recently found to have potent inhibitory effects on the growth of human breast and colon cancer.[97] Kozlowski *et al.* completed

the first total synthesis of chaetoglobin A (**25**) in 12 steps from commercially available 2,6-dimethoxytoluene.[98] Direct coupling of the highly oxidized azaphilone heterocycle was unsuccessful. Thus, a vanadium(V)-catalyzed atroposelective oxidative phenol coupling was employed using **25a** to establish the key biaryl bond of **25b** in 58% yield and 94:6 dr (**Scheme 20**). Six subsequent synthetic steps led to chaetoglobin A (**25**). While the catalyst used appears monomeric, the authors postulate that coordination of acetic acid leads to a pseudo-dimer active species.

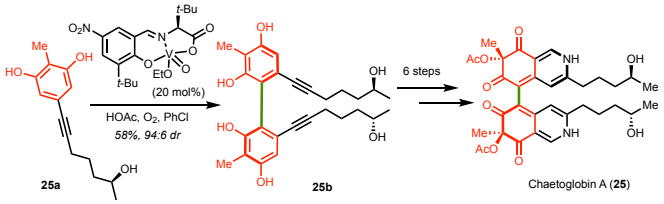

Scheme 20 Atroposelective oxidative couplings in total synthesis of chaetoglobin A.

Morphinandienone alkaloids, isolated from the opium poppy *Papaver somniferum*, have found extensive use in the medical field, often as analgesics.[99] Chemists have been trying to tackle these compounds since the elucidation of their biosynthesis, which involves an intramolecular oxidative coupling of reticuline (not shown).[60, 100-103] Prior attempts to accomplish these couplings have required the use of stoichiometric oxidants while suffering from low yields and regioselectivities.[104-106] Use of a symmetrical reticuline derivative **26a** (**Scheme 21**) reduces complexity, but there are still two regioisomeric products possible via either 8-2′/6′ or 4a-2′/6′ coupling.

In 2020, the Kozlowski group explored the selective oxidative coupling of a reticuline derivative using their method to construct phenol-dienones.[82] With catalyst **V2** (as seen in **Scheme 17a**), oxidative coupling of reticuline analogue **26a** formed (±)-salutaridine derivative (**26**) in a 71% yield via union of 4a-2′/6′ (**Scheme 21**). The alternate 8-2′/6′ coupling adduct only formed in trace quantities. These catalytic results rival the initial stoichiometric attempts from Schwartz and co-workers in the 1980s.[84]

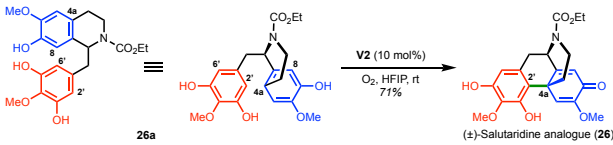

Scheme 21 Intramolecular oxidative synthesis for the synthesis of (±)-salutaridine derivative.

5.5 C–C couplings involving aryl ethers

Phenol-aryl ether oxidative couplings have been extensively reported in the literature and are often achieved with the use of hypervalent iodine oxidation chemistry. Several reviews and book chapters have outlined the use of hypervalent iodine in organic chemistry, especially in oxidative C–C bond formation of aryl ethers.[107-110] The examples shown below are not comprehensive but seek to show that these couplings can be broadly utilized, from phenol oligomers to some of the most difficult intramolecular cases. These examples also highlight some of the key advances in catalysis; namely, the use of first-row transition metals, hypervalent iodine complexes, nitrite organocatalysts, and electrochemistry. While not specifically discussed, the Wirth group recently disclosed the total synthesis of (–)-galanthamine (not shown) utilizing an electrochemical phenol-aryl ether oxidative coupling.[111]

Phlorotannins are a class of natural products typically found in algae and other aquatic plants. These compounds are oligomers of phloroglucinol and play an integral role in the structure of cell walls.[112] While their biosynthesis has yet to be elucidated, synthetic chemists have used oxidative coupling strategies to connect these compounds. The Pappo group employed sequential iron-catalyzed oxidative couplings to synthesize a variety of fucol natural products.[81] A catalytic $FeCl_3$/*t*-BuOO*t*-Bu system of the corresponding monomer provided *sym*-Me_4-difucol (**18i**, see **Scheme 16**). Using the same reaction system but with a more reactive solvent, HFIP, further cross-coupling with different equivalents of aryl ether **27a** generated Me_7-fucol (**27i**) and Me_{10}-tetrafucol A (**27ii**) in 30% and 36% yields, respectively (**Scheme 22**). This method furnishes complex natural and unnatural phlorotannin products that are typically inaccessible via prior approaches. By tuning the catalyst loading, solvent, reaction time, and oxidants, control over an oxidative coupling sequence was achieved.

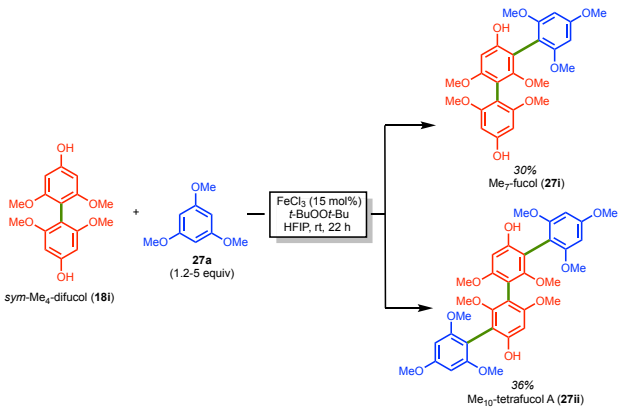

Scheme 22 Iron-catalyzed method reported by Pappo toward oligomeric natural products.

Identification of mild terminal oxidants that will generate iodine(III) *in-situ* is the key barrier to development of hypervalent iodine catalysts in oxidative coupling. Kita and co-workers found one solution to this problem in their efforts to form new C–C bonds in the oxidative coupling of phenols and aryl ethers.[113] The authors discovered that *m*-CPBA was a poor oxidant for these conditions, but *in-situ* generated bis(trifluoroacetyl) peroxide was optimal. Specifically, urea•H_2O_2 with excess TFAA led to exclusive formation of this desired peroxide which in turn generated the active iodine(III) species. Screening of other iodoarenes revealed that 4-fluoro-1-iodobenzene provided the best overall yield of 76% in the intramolecular coupling **28a** to amaryllidaceae alkaloid core **28** (**Scheme 23**).

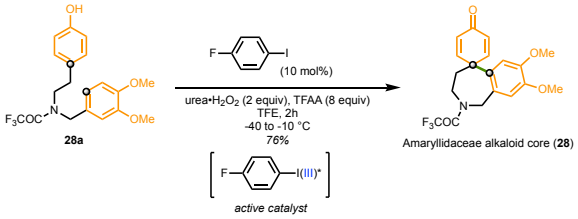

Scheme 23 Iodoarene-catalyzed oxidative coupling in accessing amaryllidaceae alkaloids.

Aporphine and morphine alkaloids have also been synthesized from aryl ether oxidative coupling approaches. Wang and co-workers reported an efficient intramolecular coupling of phenols with aryl ethers using an organocatalytic approach.[114] With a sodium nitrite catalyst and molecular oxygen as the terminal oxidant, Wang *et al.* forged new C–C bonds in **29a** derivatives to afford various aporphine alkaloid precursors (**29**) in 18–99% yields at room temperature (**Scheme 24**). NO^+ serves as the active species in the phenol single-electron oxidation, producing an NO radical which is oxidized by O_2 to complete the cycle after deprotonation. Screening of the different tethers revealed that nitrogen and amide-based linkers also performed well. The authors utilized these backbones in various Lewis acid-mediated rearrangement strategies, demonstrating promise for potential access to the aporphine alkaloid core (**29i**).

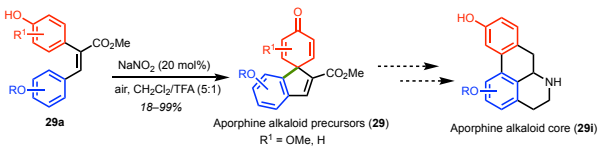

Scheme 24 Intramolecular oxidative phenol coupling with sodium nitrite to access aporphine alkaloid precursors.

(–)-Thebaine (**30**), a minor component of the opium poppy, is oft used as a synthetic precursor in the industrial-scale synthesis of other morphinandienone derivatives. Opatz and Waldvogel employed electrochemistry to access (–)-thebaine (**30**) with a regio- and diastereoselective anodic oxidative coupling.[35] As shown in **Scheme 25a**, (*R*)-**30a** was coupled using the anodic coupling conditions to furnish (+)-salutaridine analogue (**30b**) in a 59% yield. (–)-Thebaine (**30**) was achieved after six additional steps.

The following year, the Opatz and Waldvogel disclosed the total synthesis of another morphinandienone, (–)-oxycodone (**31**), with their anodic coupling system.[36] With their streamlined synthesis to (*R*)-**30a**, the authors rapidly synthesized (+)-salutaridine analogue (**30b**) with slightly modified conditions in a higher yield (69%) as seen in **Scheme 25b**. A sequence of seven subsequent steps involving a $^1O_2$ cycloaddition, hydrogenation, and removal of protecting groups led to (–)-oxycodone (**31**). Notably, the phenol groups of (*R*)-**30a** need to be protected for this strategy to succeed (see above for comparison with the unprotected phenol **Scheme 21**).

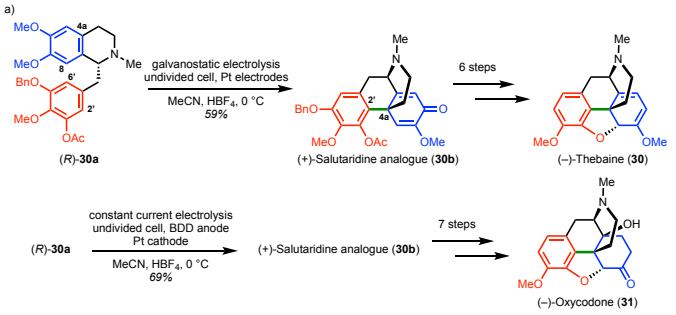

Scheme 25 Electrochemical oxidations in the syntheses of (–)-thebaine and (–)-oxycodone.

6. Catalytic C–O oxidative couplings

The formation of C–O bonds via oxidative coupling methods have proved to be much more elusive than their C–C bond counterparts. In a screening study by the Kozlowski group on aerobic oxidative coupling of phenols, a number of metal catalysts (Mn, Cr, Cu) were found to facilitate C–O bond formation from *para*-substituted phenols to provide the Pummerer ketone adducts.[23] Several reviews have focused on diaryl ether formation by means of non-oxidative couplings including many examples in natural products synthesis.[115, 116] The following examples focus on oxidative coupling to form diaryl ethers in the synthesis of natural products. Interestingly, copper catalysis has been the most successful in this context to date.

Lumb and co-workers described a series of foundational studies in which semiquinone radical intermediates obtained from copper-catalyzed oxidations were utilized. This method enabled mild *ortho*-oxygenation of phenols with molecular oxygen followed by formation of new C–O, C–N, and C–S bonds.[117] Application to intramolecular couplings allowed the formation of oxindoles via C–N bond formation.[118] In further work, Lumb *et al.* disclosed copper-catalyzed oxidative cross-couplings of *ortho*-quinones and phenols.[119] Reductive work-up accesses highly oxygenated species that are difficult to obtain by other approaches due poor regioselectivity. The authors highlighted the utility of this approach by synthesizing a xanthone natural product with known biological properties, norathyriol (**32**). Using catalytic CuCl and N,N'-dibenzylethylenediamine (DBED) under aerobic conditions, **32a** and **32b** are cross-coupled in a 76% yield after reductive work-up and acetylation to form **32c** on a gram-scale (**Scheme 26**). A series of four additional steps led to the total synthesis of norathyriol (**32**) in only six steps.

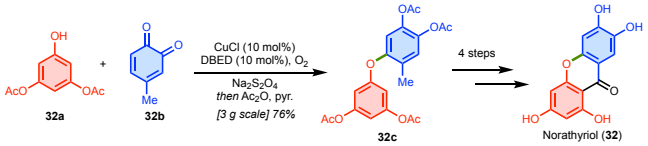

Scheme 26 Copper catalyzed cross-coupling of *ortho*-quinones with phenols.

Expanding upon this approach, Lumb and co-workers examined more complex systems including the enantioselective total synthesis of (*S,S*)-tetramethylmagnolamine (**33**).[120]

Previous syntheses had relied upon Ullman-type couplings to forge the C–O bond and these methods required high temperatures and often a stoichiometric amount of base.[121] Instead, the authors used a catalytic $CuPF_6$/DBED system to oxidatively couple **33a** in a 75% yield (**Scheme 27**). This process first begins with an *ortho* oxidation of **33a** to form the Cu(II)-semiquinone radical shown in **Scheme 27**, which then undergoes an oxidative C–O coupling. Two additional steps furnished (*S,S*)-tetramethylmagnolamine (**33**) resulting in an overall yield of 21% across seven steps. This route provides a more concise access to tetrahydroisoquinoline alkaloid dimers.

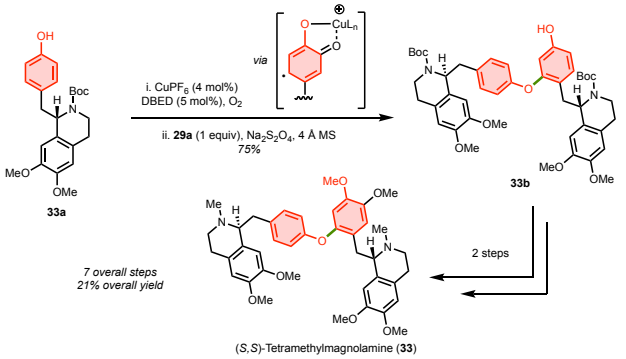

Scheme 27 Dimerization of tetrahydroisoquinoline alkaloids with Cu catalyst.

The Lumb lab also developed a copper-catalyzed oxidative coupling of phenols and catechols which enabled the total synthesis of another tetrahydroisoquinoline alkaloid (*S,S*)-thalicarpine (**34**).[122] As shown in **Scheme 28**, substrates **34a** and **34b** were oxidatively cross-coupled with CuCl and 4-MeO-Py in 76% yield after reductive work-up. (*S,S*)-Thalicarpine (**34**) was obtained after two further steps (deprotection/methylation). This key C–O bond formation served to unite two different alkaloids in a selective fashion that avoided homo-coupling. Previous work towards the synthesis of (*S,S*)-thalicarpine (**34**) from Kupchan and co-workers employed Ullman-type coupling conditions (required 140 °C) in which a Br had to be pre-installed for C–O bond formation.[123]

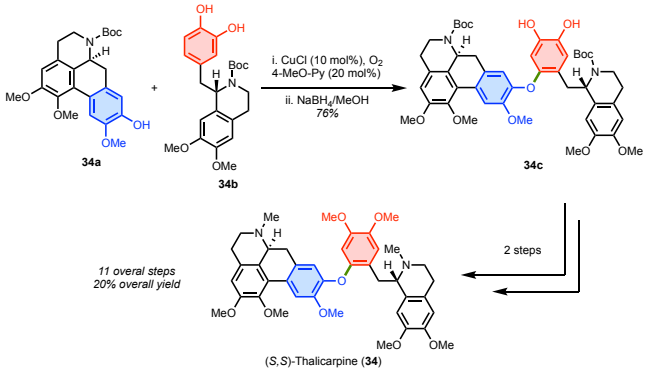

Scheme 28 Key phenol-catechol oxidative coupling step in total synthesis of (*S,S*)-thalicarpine.

While many phenolic oligomers are connected via sequential C–C bonds, a variety of phenolic trimers are connected by both C–C and C–O bonds. Pyrolaside B (**35**), a phenolic trimer natural product isolated from *Pyrola rotundifoliai/calliantha* and possessing potent anti-bacterial properties, is such a compound.[124] This natural product is composed of a A-A-A trimeric system in which all three subunits are identical but are connected via one C–C and one C–O bond. In 2020, the Kozlowski group successfully synthesized pyrolaside B (**35**) via an oxidative trimerization cascade (**Scheme 29**).[125] CuCl/pyridine and molecular oxygen oxidatively trimerize monomer **35a** to afford spiroketal **35b** in a 65% yield. Subsequent reduction and deprotection led to the first synthesis of pyrolaside B (**35**) in five steps and a 16% overall yield. This method forgoes traditional tactics (Ullman and Suzuki couplings) for assembling these types of structures that require prefunctionalization and multiple protection/deprotection steps. The authors also synthesized a variety of analogues and designed an entry to unsymmetrical trimers.

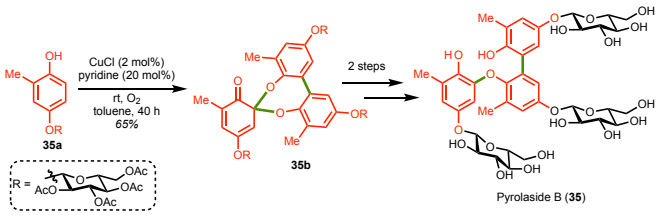

Scheme 29 Oxidative coupling trimerization cascade in the synthesis of pyrolaside B.

7. Catalytic and electrochemical alkenyl phenol oxidative couplings

Alkenyl phenols moieties exhibit rich reactivity in natural product biosynthesis and are key components of lignin, a biopolymer that provides structural support for cell walls. The large lignin waste stream from the paper industry has motivated research groups to examine lignin for multiple applications.[126, 127] Nature has devised many ways to oxidatively couple these structures to achieve a variety of diverse natural products. Upon single-electron oxidation of alkenyl phenols, radical character can delocalize to the exocyclic alkene portion allowing for a range of different coupling modalities. The Kozlowski group has highlighted the intricacies of alkenyl phenol oxidative coupling and some associated natural products in a recent review.[128] These transformations have been difficult to control; stoichiometric oxidants or enzymes result in low yields and/or poor selectivity.[129-131]

Expanding upon their repertoire of oxidative phenol couplings, Kozlowski and co-workers discovered selective methods for the oxidative homocoupling of alkenyl phenols.[132] Monomeric and dimeric vanadium catalysts were studied to bias reactivity toward specific isomers. A dimeric catalyst (similar to one from **Scheme 9**) was selective for C–O bond formation in the β-O coupling whereas a monomeric catalyst (seen in **Scheme 30**) led to the β-β coupling. Concentration and solvent also played a critical role in the selectivity where β-β coupling was promoted only in dilute acetonitrile conditions. The β-β couplings arises from C–C oxidative bond formation followed by two nucleophilic additions an XH_2 nucleophile such as H_2O or RNH_2 while β-O results from a C–O oxidative coupling and one nucleophilic addition of water.

With the optimized β-β coupling, Kozlowski and co-workers synthesized derivatives of the galbelgin core (**36**). These lignin natural products have recently emerged as key targets due to their anti-inflammatory, anti-oxidant, and anti-cancer physiological properties.[133] **Scheme 30** shows their approach where **36a** is homocoupled with a monomeric vanadium catalyst in the presence of H_2O/O_2 to furnish the galbelgin core (**36**). The method displayed good functional group tolerance with yields ranging from 17–72%, but poor diastereoselectivity (1.2–1.8:1 dr). Mechanistic experiments and high-throughput experimentation led to a rationale for why this β-β coupling is favored vs the β-O pathway. Solvents with small dipole moments (e.g. 1,4-dioxane) favored the β-O coupling, while large dipole moment solvents (e.g. acetonitrile) generated β-β coupling products. Lower concentrations led to more β-β products while higher concentrations favored the β-O coupling. Increased catalyst loadings also led to a greater selectivity for the β-O pathway over β-β. From this information, β-O coupling likely arises from a metal-bound pathway, while the β-β coupling likely occurs from a homocoupling with a free phenoxyl radical. Additionally, by utilizing other nucleophiles (e.g. anilines) instead of water, the authors were able to complete the synthesis of pyrrolidine analogues via similar β-β coupling.

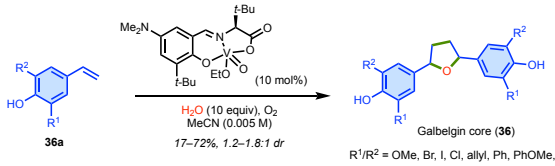

Scheme 30 Oxidative coupling of alkenyl phenols to form the galbelgin core.

Liu and co-workers reported the biomimetic oxidative cross-coupling of alkenyl phenols and phenols with an aerobic copper approach.[134] An overview of methods to construct neolignan backbones with phenol oxidative couplings has been summarized by Papaioannou *et al.*[135] Biosynthetically, these couplings are often accomplished by iron- and copper-based enzymes where homocoupling is typically observed. **Scheme 31a** displays the general strategy of Liu where catalytic $Cu(OAc)_2$/air allowed for the synthesis of natural product licarin A (**37**) in a 60% yield and >20:1 dr from commercially available **37a** in one step (**Scheme 31a**). This approach could also be used to enable cross-couplings (**Scheme 31b**). Specifically, **38a** and **38b** can be selectively cross-coupled to form 8-*O*-4′ neolignan analogues (**38i**) when EtOAc was used as solvent. With HFIP/$PhCF_3$, 8-5′ neolignan analogues (**38ii**) were obtained. However, the scope is limited to 4-amino variants of **38b** as phenols bearing 4-OMe or 3-NMe_2 were unsuccessful.

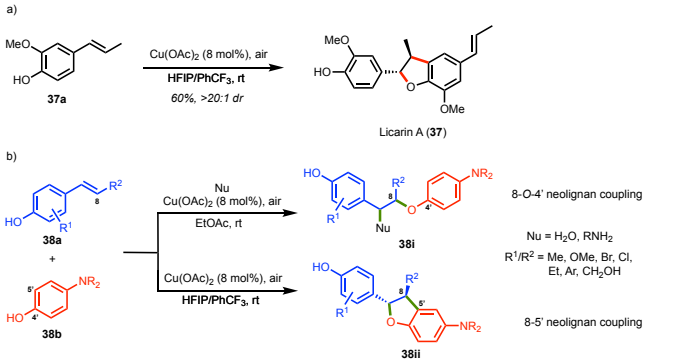

Scheme 31 Cross-coupling of phenols and alkenyl phenols in synthesis of neolignan analogues.

Alkenyl phenols can lead to a diverse array of natural products depending on the location of the alkenyl substituent relative to the phenol. Carpanone (**39**), extracted from carpano trees (*Cinnamonmum sp.*) in the south Pacific, highlights one of these alternate pathways. Biosynthetically, the assembly of carpanone (**39**) is proposed to occur in a single step, setting all five stereocenters at once.[136] In the 1970s, the Chapman group published the first biomimetic synthesis of carpanone (**39**) where they used a palladium(II) catalyst to furnish the compound in a single step with a 46% yield as a single diastereomer.[137] The observed diastereoselectivity arises from selective *endo* facial approach during an inverse-electron demand Diels-Alder reaction. This classic total synthesis highlights a rapid assembly of complexity and serves as an inspiration for highly efficient total syntheses.

Due to the very facile oxidation of the alkenyl phenol precursor to carpanone (**39**) (which even occurs slowly even under ambient conditions), many groups have achieved the oxidative synthesis of carpanone (**39**) using a variety of first-row transition metal and photochemical approaches.[138, 139] For example, Lindsley and co-workers developed a catalytic $CuCl_2$/(–)-sparteine oxidative coupling of benzoxanthenone scaffolds to afford carpanone (**39**).[140] As illustrated in **Scheme 32a**, the authors homocoupled alkenyl phenol **39a** with their optimized conditions to form **39b** which then underwent a rapid Diels-Alder [4+2] cycloaddition to form carpanone (**39**) in 91% yield as a single diastereomer. They were also able to synthesize other benzoxanthenone derivatives in high yields with this one-pot diastereoselective approach. Despite screening a range of chiral amine ligands, the authors saw little to no enantioselectivity (<5% ee).

However, the Kozlowski group recently developed a vanadium(V)-catalyzed system that induces modest levels of enantioselectivity in the constructions of benzoxanthenone backbones, a feat that was unachievable with prior methods.[141] Due to the sensitive nature of the substrate, identification of a terminal oxidant that would not directly react with the substrates proved challenging. Ultimately, AgCl was identified as an oxidant that allows the vanadium-catalyzed oxidation to occur selectively, but it was difficult to scale the reaction with this heterogenous oxidant. In this work, the authors were able to access unnatural *exo* carpanone (**39i**) in a 64% yield and 36% ee with $CuCl_2$/(–)-sparteine (**Scheme 32b**). The natural

carpanone (**39**) (*endo*) was also obtained in 20% yield, but only 6% ee. It was concluded that the vanadium catalyst provided moderate control of facial selectivity in the initial C–C bond forming event but remained coordinated for the subsequent Diels-Alder reaction directing toward an *exo* cyclization mode. A strong correlation (R^2=0.88) was found between reaction solvent dielectric and the observed enantioselectivity, where a lower solvent dielectric enhances the enantioselectivity. Studies on other derivatives led to 44–50% yields and 36–49% ee. A recent publication from the Kozlowski group detailed a photochemical oxidative coupling of phenols and alkenyl phenols using a heterogenous TiO_2 catalyst for the formation of the aforementioned natural products licarin A (**37**) and carpanone (**39**).[142]

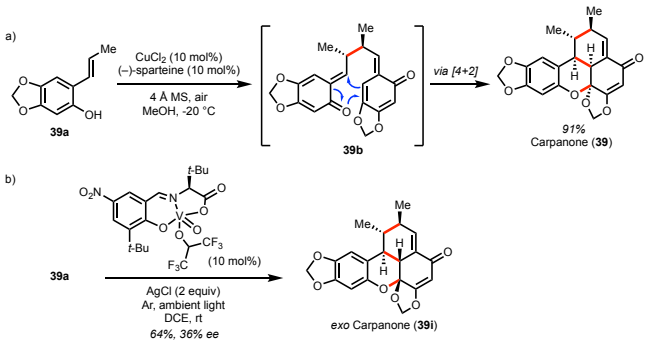

Scheme 32 Oxidative coupling approaches for synthesis of carpanone.

8. Catalytic and electrochemical oxidative coupling of phenolic-type compounds

Phenolic-type compounds can also engage in oxidative homo- and cross-coupling reactions. Such methods are often more robust than conventional cross-coupling approaches across broader areas of chemical space. Once oxidized, carbon-centered phenoxyl radicals can be captured by a variety of electrophilic species to generate complex products. Other redox active moieties, like indoles, can also oxidatively couple to form C–C bonds. This ensuing section will focus on advances in oxidative coupling of hydroxycarbazoles, amines, indoles and vinylic species including alkynes and carbonyls.

8.1 Carbazole couplings

Carbazoles are nitrogen-containing tricyclic aromatic structures that are often found in natural products and agrochemicals. Similar to naphthols, these moieties can form axially chiral biaryl products when coupled. Derivatives of carbazoles, more specifically, hydroxycarbazoles contain phenolic backbones and can participate in similar redox chemistry to phenols. Biaryl hydroxycarbazoles are typically furnished via traditional cross-coupling techniques involving pre-functionalization with a halide or other electrophiles prior to coupling. Recently, oxidative techniques have been leveraged to enable the oxidative coupling of hydroxycarbazoles.

In 2015, Kozlowski and co-workers disclosed the first vanadium-catalyzed regioselective oxidative couplings of hydroxycarbazoles using molecular oxygen as the terminal oxidant to furnish various dimeric 2-hydroxycarbazoles.[143] This study fueled their 2017 report on the asymmetric oxidative coupling of 2-hydroxycarbazoles as well as phenols.[28] With N-benzyl protecting groups, the authors oxidatively coupled **40a** derivatives to produce dimeric 2-hydroxycarbazoles (**40**) in up to 91% yields and 96% ee with monomeric vanadium(V) complexes (**Scheme 33a**). Studies into the ligand/catalyst design revealed that the addition of a Brønsted/Lewis acid increased both reactivity and enantioselectivity. Monomeric catalysts with these acid additives performed comparably to dimeric complexes. A follow-up experimental and computational study indicated that the additives help the catalysts aggregate to form "pseudo-dimeric" structures which aid in the enantioselectivity of the reaction.[144]

Takizawa and co-workers utilized a different monomeric chiral vanadium(V) catalysts to access a bis-2-hydroxycarbazole natural product, (+)-bi-2-hydroxy-3-methylcarbazole (**41**).[145] Starting from cyclohexanone and an aniline derivative, the authors achieved **41a** in two facile steps (**Scheme 33b**). The authors were able to oxidatively couple **41a** to form (+)-bi-2-hydroxy-3-methylcarbazole (**41**) in 44–70% yields and 16–21% ee. The poor enantioselectivity was attributed to the ease of rotation about the biaryl bond when the nitrogens were not protected as erosion in the enantiomeric excess was seen at room temperature.

Hydroxycarbazole natural products sorazolon E (**42a**) and (+)-sorazolon E2 (**42**), extracted from *Sorangium cellulosum* myxobacteria, have been found to possess antibacterial and cytotoxic properties against mouse fibroblasts.[146] In 2017, Sasai and Takizawa reported the first enantioselective coupling of 3-hydroxycarbazoles resulting in the total synthesis of (+)-sorazolon E2 (**42**).[147] The use of a chiral vanadium(V) catalyst **V3** enabled the homocoupling of sorazolon E (**42a**) in 71% yield and 60% ee (90% ee after recrystallization) to furnish (+)-sorazolon E2 (**42**) (**Scheme 33c**). Ultimately, the authors assembled sorazolon E (**42a**) in an efficient three step process (condensation/aromatization/C–C coupling) whereas prior art typically required up to eight steps with the use of stoichiometric toxic oxidants. It is important to note that Sasai and co-workers were able to complete this coupling in the presence of a basic nitrogen (free carbazole). These authors also reported a related enantioselective cross-coupling of 3-hydroxycarbazoles and naphthols.[148]

These authors were also able to oxidatively couple 4-hydroxycarbazoles with a dinuclear vanadium(V) complex in high yield and enantioselectivity (**Scheme 33d**).[149] Specifically, the **V3** catalyst affords 4-hydroxycarbazole dimers (**43**) under mild conditions with up to quantitative yields and 90% ee. Substrates containing hydrogen or methyl groups on the nitrogen (R^3 on **43a**) were compatible with these conditions and led to the highest enantioselectivity, but utilization of aryl, benzyl, or allyl substituents eroded selectivity. Of note, mononuclear complexes did not impart significant enantiocontrol in these reactions.

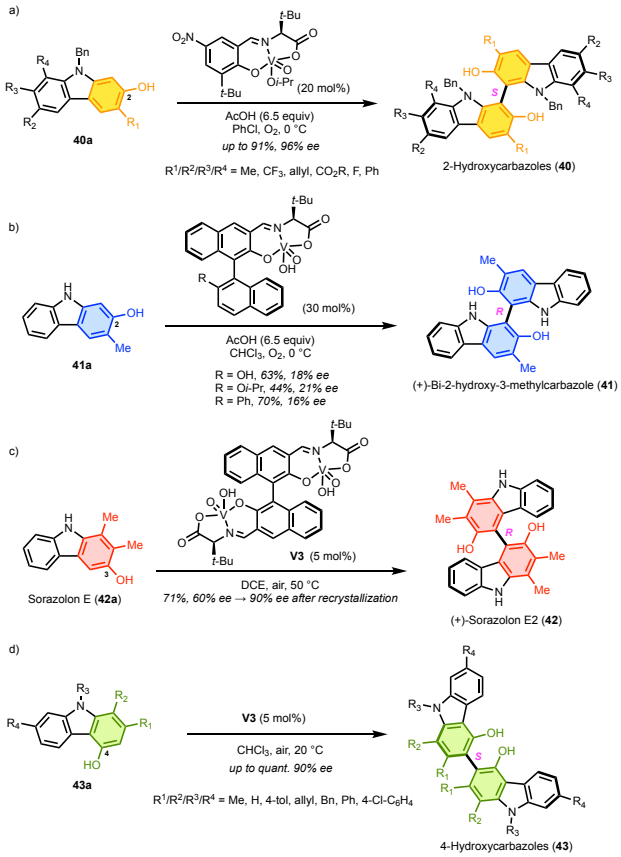

Scheme 33 Oxidative naphthol coupling to afford carbazole dimers.

8.2 Amine couplings

Lumb and co-workers disclosed the synthesis of benzoxazinone and benzoxazole backbones utilizing a biomimetic copper-catalyzed oxidative coupling of phenols and amines.[150] Similar to prior work from the Lumb group, the reactivity of an *ortho*-quinone intermediate was harnessed to forge new C–O and C–N bonds via an amine condensation in one-pot. A sterically demanding catalyst enabled regioselective *ortho*-oxygenation of symmetrical and unsymmetrical phenols to form *ortho*-aminophenols. Using $[Cu(MeCN)_4]PF_6$/DBED and molecular oxygen, the authors condensed phenol **44a** and indole amine **44b** to form **44c** which underwent lactonization to form **44d** in a 72% yield (**Scheme 34**). The benzoxazine natural product cephalandole A (**44**) was formed after subsequent de-*tert*-butylation in a 71% yield. This method proceeded with mild conditions using an earth-abundant metal (Cu) catalyst and H_2O as the only stoichiometric byproduct.

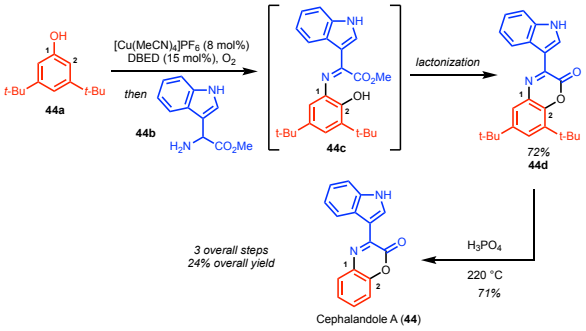

Scheme 34 Oxidative coupling of amines and phenols in the synthesis of cephalandole A.

8.3 Indole couplings

Indoles are N-heterocyclic aromatic structures with a 5-membered pyrrole fused to a benzene ring. These moieties are prevalent in biologically active natural products as well as pharmaceuticals and have remained as one of the most common scaffolds in medicinal chemistry. Indole-containing compounds have profound activity at the 5-HT serotonin receptors, including psychedelic natural products like psilocybin and ergot alkaloids which have recently garnered interest for potential treatment of depression and PTSD.[151-153]

Electrochemical methods have been pioneered to tackle difficult oxidative couplings between two unsymmetrical partners. Both phenols and indoles have sufficiently low oxidation potentials to facilitate a union in an oxidative coupling. The Harran lab utilized electrolytic conditions to accomplish an intramolecular oxidative coupling of a phenols with an indole en route to cancer therapeutic, DZ-2384 (**45**).[154] DZ-2384 (**45**) has garnered interest from the synthetic community as it showed a significant improvement in anti-cancer properties from the original natural product scaffold of (–)-diazonamide A (not shown). Conventional chemical methods involving hypervalent iodine failed to achieve the macrocyclic core of DZ-2384 (**45**) as the authors uncovered a competing oxidation of the phenolic portion (shown in red) in **45a** to a spirocyclohexadienone (not shown). Anodic conditions were devised that avoided over-oxidation of the phenol and facilitated union of the two fragments. As shown in **Scheme 35**, oxidation of **45a** at a potential of +1.6 V with portion-wise addition of $(NH_4)_2CO_3$ gave DZ-2384 (**45**) in a 35% yield and 2.3:1 dr after 56 h. Overall, the authors were able to synthesize DZ-2384 (**45**) in 13 total steps and 6% overall yield with a key oxidative coupling as the final step to achieve the macrocyclic core.

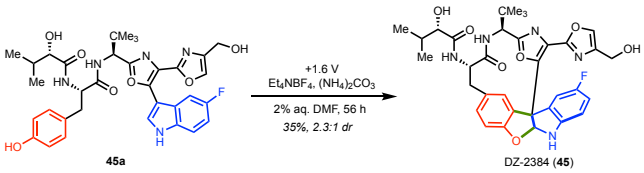

Scheme 35 Electrochemical oxidative coupling of indole and phenol to synthesize cancer therapeutic drug DZ-2384.

In a recent disclosure by Xu and co-workers, the spiroindimcin natural product family was accessed using a chemoenzymatic approach involving a biomimetic

intramolecular oxidative coupling of two indole units.[155] Spiroindimcins, isolated from deep-sea *Streptomyces* strains, are biosynthetically assembled via oxidative dimerization of tryptophan and have anti-cancer and anti-parasitic biological activities. Previous synthetic endeavors of this natural product family have relied on transition metal-catalyzed cross-coupling reactions to forge the spirocyclic skeleton.[156, 157] In a different approach, Xu *et al.* synthesized the spiroindimcin D core (**46i**) in a 35% yield using catalytic trichloroisocyanuric acid (TCCA) and the spiroindimcin A core (**46ii**) with stoichiometric NIS/$AgSbF_6$ conditions in a 98% yield (**Scheme 36**). With these regioselective 3'-2'' and 3'-4' oxidative couplings, the authors were able to synthesize (±)-spiroindimcin A, D, G, and H (not shown) after one or two additional synthetic procedures. The common intermediate **46a** was produced via an enzymatic dimerization of L-tryptophan.

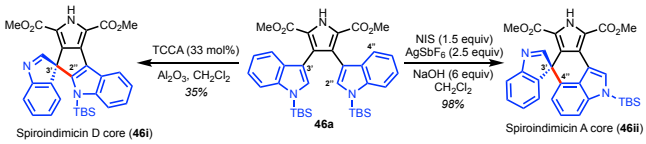

Scheme 36 Total synthesis of spiroindimcin cores via indole oxidative coupling.

8.4 Alkyne and alkene couplings

The use of low-energy visible light has emerged as a powerful synthetic technique to furnish new chemical bonds with mild, selective transformations. The Hwang lab reported the oxidative coupling of phenols and terminal alkynes using photocatalytic conditions and an earth-abundant copper catalyst.[158] In the presence of O_2, C≡C triple bonds are cleaved to assemble alkyl and aryl ketones, which are valuable functional groups in natural products as well as useful synthetic intermediates. In this reaction, the phenol is first oxidized to the *para*-quinone with $CuCl/O_2$ and then undergoes a Paterno-Buchi [2+2] cycloaddition with a Cu(II)-acetylide which undergoes subsequent ring opening and addition with O_2 to form the product after loss of CO_2 (**Scheme 37a**). As suggested by the mechanism, the scope is limited to phenols with open *para* positions. This method allowed the authors to synthesize two pharmaceuticals in a high yielding two-step process. Alkyne **47a** and phenol **47b** were coupled using the photocatalytic conditions in a 82% yield and then subsequently engaged in an S_N2 reaction to afford pitofenone (**47**) in a 72% overall yield (**Scheme 37b**). A similar approach was taken to form fenofibrate (**48**), a cholesterol drug, using **48a** and **47b** in a 76% overall yield (**Scheme 37c**).

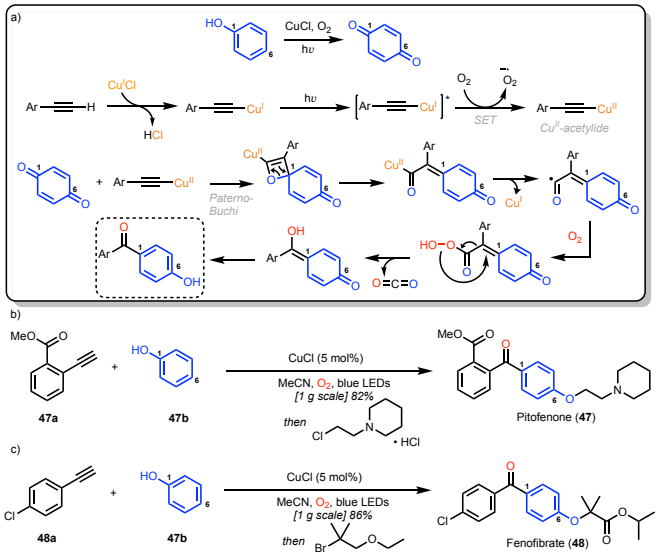

Scheme 37 Photocatalytic oxidative coupling of phenols and terminal alkynes.

In 2013, Pappo and co-workers developed an iron-catalyzed oxidative cross-coupling of phenols and alkenes for the construction of 2,3-dibenzofurans (**49**).[159] These moieties are present in a plethora of natural products and it is proposed that nature constructs these backbones in a similar oxidative fashion.[160] Previous methods have been established for the synthesis of 2,3-dibenzofurans (**49**), but they often rely upon stoichiometric metal oxidants with poor selectivity outcomes. Using a $FeCl_3$/*t*-BuOO*t*-Bu/DCE system, the authors were able to couple a variety of phenols and naphthols (**49a**) with styrene and stilbene derivatives (**49b**) to furnish 2,3-dibenzofurans (**49**) in 27–94% yields (**Scheme 38**). For further examples of the use of oxidative couplings in the assembly of dihydrobenzofuran natural products, see review by Zhao *et al*.[161]

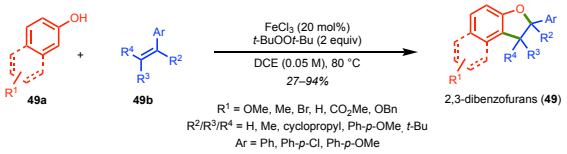

Scheme 38 Photocatalytic oxidative coupling of phenols and terminal alkynes.

8.5 1,3-Dicarbonyl couplings

A subsequent study from Pappo *et al.* in 2015 examined catalytic oxidative coupling of phenols and β-dicarbonyls to furnish benzofurans.[162] The authors observed a dramatic enhancement in cross-coupling selectivity with fluoroalcohol solvents (HFIP/TFE) which is hypothesized to arise from their ability to stabilize radical cation intermediates. Partners **50a** and **50b** were oxidatively coupled using a $Fe(ClO_4)_3$ hydrate catalyst in TFE/DCE in 40% yield (**Scheme 39**). Three additional synthetic procedures resulted in the first total synthesis of natural product 2''-dehydroxycalodenin B (**50**) in a 17% overall yield. While a stoichiometric loading of catalyst was used in the total synthesis, the substrate scope disclosed by Pappo and co-workers used only a 10 mol% loading.

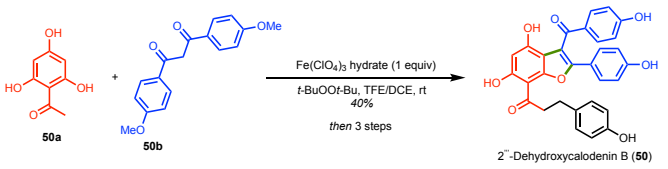

Scheme 39 Oxidative coupling of phenols and β-dicarbonyl compounds in the synthesis of 2‴-dehydroxycalodenin B.

Expanding upon their work in iron-catalyzed oxidative couplings of phenols and β-dicarbonyls, Pappo *et al.* were able to access coumestrol analogues (**51**) for a structural activity relationship (SAR) study against breast cancer cell lines.[163] In their synthesis of a library of coumestrol derivatives (**51**), the Pappo group leveraged a two-step approach involving the assembly of a 3-ester benzofuran intermediate followed by lactone formation via an intramolecular esterification. **Scheme 39** illustrates their approach in which **51a** and **51b** are oxidatively coupled to form **51c** derivatives in 51–77% yields using $FeCl_3$ and *t*-BuOO*t*-Bu. Subsequent BBr_3 deprotection of the methoxy groups and lactonization led to coumestrol analogues (**51**) in 67–97% yields. For the oxidative coupling, the use of molecular oxygen as the terminal oxidant led to inferior yields in comparison to *t*-BuOO*t*-Bu. Additionally, the authors were able to complete the gram scale total synthesis of natural product coumestrol (not shown) in a 59% overall yield.

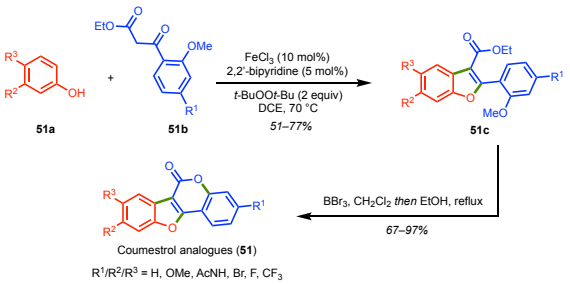

Scheme 40 Synthesis of coumestrol derivatives via oxidative coupling of β-ketoesters with phenols.

The Pappo group also reported a key advance with the stereoselective oxidative coupling of 2-naphthols with chiral β-ketoesters using a chiral iron phosphate complex to synthesize polycyclic hemiacetal analogues.[164] Benzofuran-based polycyclic acetals are key backbones in many natural products with promising biological properties.[165] The authors screened a diverse set of phosphoric acid ligands with an $Fe(ClO_4)_3$ hydrate catalyst to achieve both high yield and diastereoselectivity. Mechanistic studies revealed that the active catalyst was an iron monophosphate complex. **Scheme 40** highlights the optimized conditions using an (*R*)-BNPH ligand in $PhCF_3$/HFIP to couple derivatives of **52a** and **52b** to form polycyclic hemiacetals (**52**) in 57–79% yields and up to 90:10 dr. Motivated by this work, Sasai and Takizawa disclosed a catalytic enantioselective oxidative coupling between 3-hydroxycarbazoles and achiral β-ketoesters with their vanadium(V) catalysts.[148]

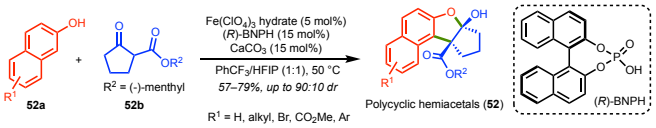

Scheme 41 Asymmetric oxidative coupling of 2-naphthols and β-ketoesters with iron phosphate catalyst.

The Pappo lab also developed an iron-catalyzed oxidative coupling of naphthols/phenols with β-ketoesters to favor the formation of spirolactones over polycyclic hemiacetals.[166] The authors discovered that elevated temperatures (above 70 °C) facilitate the trans-esterification step required to form spirolactones and avoid formation of polycyclic hemiacetals using traditional $FeCl_3$/*t*-BuOO*t*-Bu/DCE conditions. The utility of this method was highlighted in the biomimetic synthesis of the lachnanthospirone core (**53**), a pigment isolated from *Lachnanthes tinctoria*. The original isolation paper hypothesized that lachnanthospirone (not shown) could be biosynthetically assembled via an oxidative coupling of a phenol and β-ketoester.[167] To probe the synthetic feasibility, Pappo and co-workers coupled **53a** and **53b** using their optimized oxidative conditions to afford the lachnanthospirone core (**53**) in a 43% yield (**Scheme 41**) with sequential C–C and C–O bond formation.

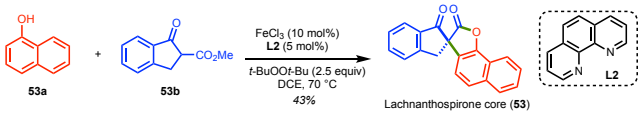

Scheme 42 Iron-catalyzed coupling of β-ketoesters with naphthols in synthesis of lachnanthospirone core.

9. Concluding remarks

In conclusion, oxidative phenol couplings have significantly aided synthetic chemists in their quest to synthesize elusive natural products. Tremendous strides have been made within the last decade using innovate chemistries to push the boundaries and reach new chemical space. These powerful bond-forming reactions, requiring no prefunctionalization, have found wide applications with coupling diverse partners.

Chemical approaches utilizing stoichiometric oxidants have fared well in the assembly of complex natural products, but their ultimate utility is limited by the presence of sensitive functional groups. Enzymatic oxidative couplings have been recently leveraged to conduct bench-top reactions with biological precision. Catalytic oxidative methods have combined atom economy, reaction efficiency, and functional group tolerance to achieve selective transformations in furnishing natural products. Of the transition metal catalysts, those derived from iron, vanadium, copper, and chromium have emerged as the most successful catalyst types in the field. Electrochemistry has gained prominence in oxidative coupling by succeeding under mild conditions and with high selectivity. Additionally, oxidative photoredox chemistry has recently proven advantageous in oxidative phenol couplings by using low-energy visible light.

While the regioselectivity of phenol homocoupling has been carefully analyzed in several studies, regioselective cross-coupling approaches remain a challenge and often rely upon the

use of blocking/activating groups. The installation and subsequent removal of such moieties increases synthetic step counts. Discovering approaches that reduce these inefficiencies and allow direct regioselective cross-couplings will lead to shorter and even more efficient syntheses. Expanding phenol oxidative couplings to new heteroarenes is also of interest to the community. These bonds are often forged by stoichiometric Lewis acids and transition metals, which can create roadblocks in drug development on industrial scale. Overall, the oxidative coupling of phenols and phenolic-type compounds have enabled synthetic chemists to mimic biological pathways in the synthesis of complex natural products. Further advances will enhance efficiency and allow for use with non-natural substrates to access greater portions of chemical space.

10. Conflicts of interest

There are no conflicts to declare.

11. Acknowledgements

We are grateful to the NSF (CHE2102626) and the NIH (R35 GM131902) for financial support of this research.

12. References

1. R. Pummerer and F. Frankfurter, *Ber. Dtsch. Chem. Ges.*, 1914, **47**, 1472-1493.
2. A. I. Scott, *Q. Rev. Chem. Soc.*, 1965, **19**, 1.
3. S. P. Roche and J. A. Porco, *Angew. Chem. Int. Ed.*, 2011, **50**, 4068-4093.
4. R. Fan, Q. Ding and Y. Ye, *Synthesis*, 2012, **45**, 1-16.
5. C. J. Huck, Y. D. Boyko and D. Sarlah, *Nat. Prod. Rep.*, 2022, **39**, 2231-2291.
6. C. H. Hassall and J. R. Lewis, *J. Chem. Soc.*, 1961, 2312-2315.
7. D. G. O'Donovan and H. Horan, *J. Chem. Soc. C*, 1969, 1737-1739.
8. K. Woithe, N. Geib, K. Zerbe, D. B. Li, M. Heck, S. Fournier-Rousset, O. Meyer, F. Vitali, N. Matoba, K. Abou-Hadeed and J. A. Robinson, *J. Am. Chem. Soc.*, 2007, **129**, 6887-6895.
9. S. Tang and G. Vincent, *Chem. Eur. J.*, 2021, **27**, 2612-2622.
10. C. S. Yeung and V. M. Dong, *Chem. Rev.*, 2011, **111**, 1215-1292.
11. M. C. Kozlowski, *Acc. Chem. Res.*, 2017, **50**, 638-643.
12. V. Arkley, F. M. Dean, A. Robertson and P. Sidisunthorn, *J. Chem. Soc.*, 1956, 2322-2328.
13. H. Taguchi, U. Sankawa and S. Shibata, *Chem. Pharm. Bull.*, 1969, **17**, 2054-2060.
14. D. H. R. Barton, A. M. Deflorin and O. E. Edwards, *J. Chem. Soc.*, 1956, 530-534.
15. R. Pummerer, H. Puttfarcken and P. Schopflocher, *Ber. Dtsch. Chem. Ges.*, 1925, **58**, 1808-1820.
16. D. H. R. Barton, A. M. Deflorin and O. E. Edwards, *Chem. Ind.*, 1955, 1039-1040.
17. D. H. R. Barton and T. Cohen, in *Fetschrift* ed. A. Stoll, Basel, Birkhauser, 1957, pp. 117-143.
18. J. Wu and M. C. Kozlowski, *ACS Catal.*, 2022, **12**, 6532-6549.
19. M. C. Kozlowski, B. J. Morgan and E. C. Linton, *Chem. Soc. Rev.*, 2009, **38**, 3193.
20. A. Libman, H. Shalit, Y. Vainer, S. Narute, S. Kozuch and D. Pappo, *J. Am. Chem. Soc.*, 2015, **137**, 11453-11460.
21. H. Shalit, A. Libman and D. Pappo, *J. Am. Chem. Soc.*, 2017, **139**, 13404-13413.
22. H. Shalit, A. Dyadyuk and D. Pappo, *J. Org. Chem.*, 2019, **84**, 1677-1686.
23. Y. E. Lee, T. Cao, C. Torruellas and M. C. Kozlowski, *J. Am. Chem. Soc.*, 2014, **136**, 6782-6785.
24. Y. Nieves-Quinones, T. J. Paniak, Y. E. Lee, S. M. Kim, S. Tcyrulnikov and M. C. Kozlowski, *J. Am. Chem. Soc.*, 2019, **141**, 10016-10032.
25. K. V. N. Esguerra, Y. Fall, L. Petitjean and J.-P. Lumb, *J. Am. Chem. Soc.*, 2014, **136**, 7662-7668.
26. F. Schön, E. Kaifer and H. J. Himmel, *Chem. Eur. J.*, 2019, **25**, 8279-8288.
27. S. Takizawa, J. Kodera, Y. Yoshida, M. Sako, S. Breukers, D. Enders and H. Sasai, *Tetrahedron*, 2014, **70**, 1786-1793.
28. H. Kang, Y. E. Lee, P. V. G. Reddy, S. Dey, S. E. Allen, K. A. Niederer, P. Sung, K. Hewitt, C. Torruellas, M. R. Herling and M. C. Kozlowski, *Org. Lett.*, 2017, **19**, 5505-5508.
29. K. A. Niederer, P. H. Gilmartin and M. C. Kozlowski, *ACS Catal.*, 2020, **10**, 14615-14623.
30. A. Kumar, H. Sasai and S. Takizawa, *Acc. Chem. Res.*, 2022, **55**, 2949-2965.
31. J.-P. Lumb and K. Esguerra, *Synlett*, 2015, **26**, 2731-2738.
32. A. Kirste, G. Schnakenburg, F. Stecker, A. Fischer and S. R. Waldvogel, *Angew. Chem. Int. Ed.*, 2010, **49**, 971-975.
33. A. Kirste, G. Schnakenburg and S. R. Waldvogel, *Org. Lett.*, 2011, **13**, 3126-3129.
34. A. Kirste, B. Elsler, G. Schnakenburg and S. R. Waldvogel, *J. Am. Chem. Soc.*, 2012, **134**, 3571-3576.
35. A. Lipp, D. Ferenc, C. Gütz, M. Geffe, N. Vierengel, D. Schollmeyer, H. J. Schäfer, S. R. Waldvogel and T. Opatz, *Angew. Chem. Int. Ed.*, 2018, **57**, 11055-11059.
36. A. Lipp, M. Selt, D. Ferenc, D. Schollmeyer, S. R. Waldvogel and T. Opatz, *Org. Lett.*, 2019, **21**, 1828-1831.
37. M. Geffe and T. Opatz, *Org. Lett.*, 2014, **16**, 5282-5285.
38. S. A. Baker Dockrey, A. L. Lukowski, M. R. Becker and A. R. H. Narayan, *Nat. Chem.*, 2018, **10**, 119-125.
39. A. Rodríguez Benítez, S. E. Tweedy, S. A. Baker Dockrey, A. L. Lukowski, T. Wymore, D. Khare, C. L. Brooks, B. A. Palfey, J. L. Smith and A. R. H. Narayan, *ACS Catal.*, 2019, **9**, 3633-3640.
40. L. E. Zetzsche and A. R. H. Narayan, *Nat. Rev. Chem.*, 2020, **4**, 334-346.
41. L. E. Zetzsche, J. A. Yazarians, S. Chakrabarty, M. E. Hinze, L. A. M. Murray, A. L. Lukowski, L. A. Joyce and A. R. H. Narayan, *Nature*, 2022, **603**, 79-85.
42. W. Hüttel and M. Müller, *ChemBioChem*, 2007, **8**, 521-529.
43. L. S. Mazzaferro, W. Hüttel, A. Fries and M. Müller, *J. Am. Chem. Soc.*, 2015, **137**, 12289-12295.
44. W. Hüttel and M. Müller, *Nat. Prod. Rep.*, 2021, **38**, 1011-1043.
45. S. A. Baker Dockrey and A. R. H. Narayan, *Org. Lett.*, 2020, **22**, 3712-3716.
46. L. Péault, A. Planchat, P. Nun, E. Le Grognec and V. Coeffard, *J. Org. Chem.*, 2021, **86**, 18192-18203.

47. M. C. Carson, B. J. Orzolek and M. C. Kozlowski, *Org. Lett.*, 2022, **24**, 7250-7254.
48. A. Afanasenko, A. Kavun, D. Thomas and C. J. Li, *Chem. Eur. J.*, 2022, **28**.
49. N. Denizot, A. Pouilhès, M. Cucca, R. Beaud, R. Guillot, C. Kouklovsky and G. Vincent, *Org. Lett.*, 2014, **16**, 5752-5755.
50. E. Poupon, L. Evanno, G. Vincent, N. Denizot, D. Lachkar and C. Kouklovsky, *Synthesis*, 2018, **50**, 4229-4242.
51. K. Morimoto, *Chem. Pharm. Bull.*, 2019, **67**, 1259-1270.
52. M. Tissot, R. J. Phipps, C. Lucas, R. M. Leon, R. D. M. Pace, T. Ngouansavanh and M. J. Gaunt, *Angew. Chem. Int. Ed.*, 2014, **53**, 13498-13501.
53. D. F. Taber, T. D. Neubert and A. L. Rheingold, *J. Am. Chem. Soc.*, 2002, **124**, 12416-12417.
54. P. Magnus, N. Sane, B. P. Fauber and V. Lynch, *J. Am. Chem. Soc.*, 2009, **131**, 16045-16047.
55. A. Richieu, P. A. Peixoto, L. Pouységu, D. Deffieux and S. Quideau, *Angew. Chem. Int. Ed.*, 2017, **156**, 13833-13837.
56. N. Michihata, Y. Kaneko, Y. Kasai, K. Tanigawa, T. Hirokane, S. Higasa and H. Yamada, *J. Org. Chem.*, 2013, **78**, 4319-4328.
57. S. Wakamori, R. Osada, S. Matsumoto, R. Kusuki and K. Murakami, *Org. Lett.*, 2022, **24**, 8130-8135.
58. D. S. Peters, F. E. Romesberg and P. S. Baran, *J. Am. Chem. Soc.*, 2018, **140**, 2072-2075.
59. Z.-W. Guo, G. M. Salamonczyk, K. Han, K. Machiya and C. J. Sih, *J. Org. Chem.*, 1997, **62**, 6700-6701.
60. X. Zhang and S. Li, *Nat. Prod. Rep.*, 2017, **34**, 1061-1089.
61. W.-T. Liu, R. D. Kersten, Y.-L. Yang, B. S. Moore and P. C. Dorrestein, *J. Am. Chem. Soc.*, 2011, **133**, 18010-18013.
62. C. Molinaro, Y. Kawasaki, G. Wanyoike, T. Nishioka, T. Yamamoto, B. Snedecor, S. J. Robinson and F. Gosselin, *J. Am. Chem. Soc.*, 2022, **144**, 14838-14845.
63. V. G. Dumas, L. A. Defelipe, A. A. Petruk, A. G. Turjanski and M. A. Marti, *Proteins: Struct. Funct. Genet.*, 2014, **82**, 1004-1021.
64. J. R. Cochrane, J. M. White, U. Wille and C. A. Hutton, *Org. Lett.*, 2012, **14**, 2402-2405.
65. X. Zhu, C. C. Mcatee and C. S. Schindler, *Org. Lett.*, 2018, **20**, 2862-2866.
66. C. Gil Girol, K. M. Fisch, T. Heinekamp, S. Günther, W. Hüttel, J. Piel, A. A. Brakhage and M. Müller, *Angew. Chem. Int. Ed.*, 2012, **51**, 9788-9791.
67. L. E. Zetzsche, S. Chakrabarty and A. R. H. Narayan, *ACS Chem. Bio.*, 2022, **17**, 2986-2992.
68. E. E. Podlesny and M. C. Kozlowski, *Org. Lett.*, 2012, **14**, 1408-1411.
69. E. E. Podlesny and M. C. Kozlowski, *J. Org. Chem.*, 2013, **78**, 466-476.
70. J. Dai, Y. Liu, Y.-D. Zhou and D. G. Nagle, *J. Nat. Prod.*, 2007, **70**, 1824-1826.
71. E. E. Podlesny and M. C. Kozlowski, *J. Nat. Prod.*, 2012, **75**, 1125-1129.
72. M. Ben-Lulu, E. Gaster, A. Libman and D. Pappo, *Angew. Chem. Int. Ed.*, 2020, **59**, 4835-4839.
73. M. Phillips, *Science*, 1931, **73**, 568-570.
74. K. Iwahara, Y. Honda, T. Watanabe and M. Kuwahara, *Appl. Microbiol. Biotechnol.*, 2000, **54**, 104-111.
75. J. Wang, A. Galgoci, S. Kodali, K. B. Herath, H. Jayasuriya, K. Dorso, F. Vicente, A. González, D. Cully, D. Bramhill and S. Singh, *J. Biol. Chem.*, 2003, **278**, 44424-44428.
76. Y. S. Park, C. I. Grove, M. González-López, S. Urgaonkar, J. C. Fettinger and J. T. Shaw, *Angew. Chem. Int. Ed.*, 2011, **50**, 3730-3733.
77. J. Shaw, C. Grove and J. Fettinger, *Synthesis*, 2012, **44**, 362-371.
78. J. Feng, X. B. Yang, S. Lang, J. Zhang and X. Q. Yu, *Tetrahedron Lett.*, 2013, **54**, 355-357.
79. X. Wu, T. Iwata, A. Scharf, T. Qin, K. D. Reichl and J. A. Porco, *J. Am. Chem. Soc.*, 2018, **140**, 5969-5975.
80. O. Hollóczki, A. Berkessel, J. Mars, M. Mezger, A. Wiebe, S. R. Waldvogel and B. Kirchner, *ACS Catal.*, 2017, **7**, 1846-1852.
81. V. Vershinin, A. Dyadyuk and D. Pappo, *Tetrahedron*, 2017, **73**, 3660-3668.
82. P. H. Gilmartin and M. C. Kozlowski, *Org. Lett.*, 2020, **22**, 2914-2919.
83. M. A. Schwartz, B. F. Rose, R. A. Holton, S. W. Scott and B. Vishnuvajjala, *J. Am. Chem. Soc.*, 1977, **99**, 2571-2578.
84. M. A. Schwartz and M. F. Zoda, *J. Org. Chem.*, 1981, **46**, 4623-4625.
85. M. Schubert, K. Wehming, A. Kehl, M. Nieger, G. Schnakenburg, R. Fröhlich, D. Schollmeyer and S. R. Waldvogel, *Eur. J. Org. Chem.*, 2016, **2016**, 60-63.
86. H. Hamamoto, G. Anilkumar, H. Tohma and Y. Kita, *Eur. J. Chem.*, 2002, **8**, 5377-5383.
87. G. Blasko and G. A. Cordell, *Heterocycles*, 1988, **27**, 445-452.
88. M.-M. Li, Y. Wu and B. Liu, *Org. Lett.*, 2019, **21**, 575-578.
89. M. Greenberg, M. Dodds and M. Tian, *J. Agric. Food Chem.*, 2008, **56**, 11151-11156.
90. Y. Sakaue, H. Domon, M. Oda, S. Takenaka, M. Kubo, Y. Fukuyama, T. Okiji and Y. Terao, *Microbiol. Immunol.*, 2016, **60**, 10-16.
91. a) C. R. Ochoa, H. F. Roenfanz and M. C. Kozlowski, *ChemMedChem*, 2022, **17,** e202100783. b) H. F. Roenfanz C. R. Ochoa and M. C. Kozlowski, *ChemMedChem*, 2023, **18,** e202200521.
92. S. Jaracz, M. C. Kozlowski, Y. E. Lee, S. M. Kim, WO/2017/070568, Improved Synthesis of Honokiol, 2017 Apr 27.
93. B. V. S. Reddy, R. N. Rao, N. S. S. Reddy, R. Somaiah, J. S. Yadav and R. Subramanyam, *Tetrahedron Lett.*, 2014, **55**, 1049-1051.
94. J. Srinivas, P. P. Singh, Y. K. Varma, I. Hyder and H. M. S. Kumar, *Tetrahedron Lett.*, 2014, **55**, 4295-4297.
95. K. Harada, C. Arioka, A. Miyakita, M. Kubo and Y. Fukuyama, *Tetrahedron Lett.*, 2014, **55**, 6001-6003.
96. A. E. Solinski, C. Ochoa, Y. E. Lee, T. Paniak, M. C. Kozlowski and W. M. Wuest, *ACS Infect. Dis.*, 2018, **4**, 118-122.
97. H. Ming Ge, W. Yun Zhang, G. Ding, P. Saparpakorn, Y. Chun Song, S. Hannongbua and R. Xiang Tan, *Chem. Commun.*, 2008, **45**, 5978-5980.
98. H. Kang, C. Torruellas, J. Liu and M. C. Kozlowski, *Org. Lett.*, 2018, **20**, 5554-5558.
99. K. L. Stuart, *Chem. Rev.*, 1971, **71**, 47-72.
100. H. Hamamoto, Y. Shiozaki, H. Nambu, K. Hata, H. Tohma and Y. Kita, *Eur. J. Chem.*, 2004, **10**, 4977-4982.
101. H. Hara, S. Komoriya, T. Miyashita and O. Hoshino, *Tetrahedron-Asymmetry*, 1995, **6**, 1683-1692.

102. R. Stadler, T. M. Kutchan, S. Loeffler, N. Nagakura, B. Cassels and M. H. Zenk, *Tetrahedron Lett.*, 1987, **28**, 1251-1254.
103. D. S. Bhakuni and S. Jain, *J. Chem. Soc., Perkin Trans. 1*, 1988, 1447-1449.
104. M. A. Schwartz and P. P. T. Kim, *J. Org. Chem.*, 1988, **53**, 2318-2322.
105. M. A. Schwartz, *Synth. Commun.*, 1973, **3**, 33-35.
106. D. G. Vanderlaan and M. A. Schwartz, *J. Org. Chem.*, 1985, **50**, 743-747.
107. Y. Qin, L. Zhu and S. Luo, *Chem. Rev.*, 2017, **117**, 9433-9520.
108. A. Yoshimura and V. V. Zhdankin, *Chem. Rev.*, 2016, **116**, 3328-3435.
109. T. Dohi and Y. Kita, *PATAI'S Chemistry of Functional Groups*, 2018, DOI: 10.1002/9780470682531.pat0952, 1-84.
110. S. Quideau, D. Deffieux and L. Pouységu, *Comprehensive Organic Synthesis II*, 2014, DOI: 10.1016/B978-0-08-097742-3.00318-9, 656-740.
111. Z. Xiong, F. Weidlich, C. Sanchez and T. Wirth, *Org. Biomol. Chem.*, 2022, **20**, 4123-4127.
112. H. Bridi, G. D. Meirelles and G. L. von Poser, *Phytochemistry*, 2018, **155**, 203-232.
113. T. Dohi, Y. Minamitsuji, A. Maruyama, S. Hirose and Y. Kita, *Org. Lett.*, 2008, **10**, 3559-3562.
114. B. Su, M. Deng and Q. Wang, *Org. Lett.*, 2013, **15**, 1606-1609.
115. G. Evano, J. Wang and A. Nitelet, *Org. Chem. Front.*, 2017, **4**, 2480-2499.
116. E. N. Pitsinos, V. P. Vidali and E. A. Couladouros, *Eur. J. Org. Chem.*, 2011, **2011**, 1207-1222.
117. K. V. N. Esguerra, Y. Fall and J.-P. Lumb, *Angew. Chem. Int. Ed.*, 2014, **53**, 5877-5881.
118. Z. Huang, M. S. Askari, K. V. N. Esguerra, T.-Y. Dai, O. Kwon, X. Ottenwaelder and J.-P. Lumb, *Chem. Sci.*, 2016, **7**, 358-369.
119. Z. Huang and J.-P. Lumb, *Angew. Chem. Int. Ed.*, 2016, **55**, 11543-11547.
120. Z. Huang, X. Ji and J.-P. Lumb, *Org. Lett.*, 2019, **21**, 9194-9197.
121. N. Blank and T. Opatz, *J. Org. Chem.*, 2011, **76**, 9777-9784.
122. W. Xu, Z. Huang, X. Ji and J.-P. Lumb, *ACS Catal.*, 2019, **9**, 3800-3810.
123. S. M. Kupchan, A. J. Liepa, V. Kameswaran and K. Sempuku, *J. Am. Chem. Soc.*, 1973, **95**, 2995-3000.
124. J. Chang and T. Inui, *Chem. Pharm. Bull.*, 2005, **53**, 1051-1053.
125. W. C. Neuhaus and M. C. Kozlowski, *Angew. Chem. Int. Ed.*, 2020, **59**, 7842-7847.
126. E. P. Feofilova and I. S. Mysyakina, *Appl. Biochem. Microbiol.*, 2016, **52**, 573-581.
127. Z. Sun, B. Fridrich, A. De Santi, S. Elangovan and K. Barta, *Chem. Rev.*, 2018, **118**, 614-678.
128. W. C. Neuhaus, A. L. Jemison and M. C. Kozlowski, *Org. Biomol. Chem.*, 2021, **19**, 8205-8226.
129. V. Nair, J. Mathew, P. P. Kanakamma, S. B. Panicker, V. Sheeba, S. Zeena and G. K. Eigendorf, *Tetrahedron Lett.*, 1997, **38**, 2191-2194.
130. P. Gavezzotti, C. Navarra, S. Caufin, B. Danieli, P. Magrone, D. Monti and S. Riva, *Adv. Synth. Catal.*, 2011, **353**, 2421-2430.
131. T. Kishimoto, N. Takahashi, M. Hamada and N. Nakajima, *J. Agric. Food Chem.*, 2015, **63**, 2277-2283.
132. W. C. Neuhaus, A. L. Jemison and M. C. Kozlowski, *ACS Catal.*, 2019, **9**, 11067-11073.
133. J.-Y. Pan, S.-L. Chen, M.-H. Yang, J. Wu, J. Sinkkonen and K. Zou, *Nat. Prod. Rep.*, 2009, **26**, 1251.
134. K. Dong, C.-Y. Zhao, X.-J. Wang, L.-Z. Wu and Q. Liu, *Org. Lett.*, 2021, **23**, 2816-2820.
135. G. E. Magoulas and D. Papaioannou, *Molecules*, 2014, **19**, 19769-19835.
136. E. Poupon and B. Nay, *Biomimetic Organic Synthesis*, 2011, DOI: 10.1002/9783527634606.
137. O. L. Chapman, M. R. Engel, J. P. Springer and J. C. Clardy, *J. Am. Chem. Soc.*, 1971, **93**, 6696-6698.
138. M. Matsumoto and K. Kuroda, *Tetrahedron Lett.*, 1981, **22**, 4437-4440.
139. K. Nihon, *Bull. Chem. Soc. Jpn.*, 1992, **65**, 1662-1664.
140. R. N. Daniels, O. O. Fadeyi and C. W. Lindsley, *Org. Lett.*, 2008, **10**, 4097-4100.
141. W. C. Neuhaus and M. C. Kozlowski, *Chem. Asian J.*, 2020, **15**, 1039-1043.
142. J. Wu and M. C. Kozlowski, *Org. Lett.*, 2023, **25**, 907-911.
143. L. Liu, P. J. Carroll and M. C. Kozlowski, *Org. Lett.*, 2015, **17**, 508-511.
144. H. Kang, M. R. Herling, K. A. Niederer, Y. E. Lee, P. Vasu Govardhana Reddy, S. Dey, S. E. Allen, P. Sung, K. Hewitt, C. Torruellas, G. J. Kim and M. C. Kozlowski, *J. Org. Chem.*, 2018, **83**, 14362-14384.
145. M. Sako, A. Sugizaki and S. Takizawa, *Bioorg. Med. Chem. Lett.*, 2018, **28**, 2751-2753.
146. J. Herrmann, A. A. Fayad and R. Müller, *Nat. Prod. Rep.*, 2017, **34**, 135-160.
147. M. Sako, K. Ichinose, S. Takizawa and H. Sasai, *Chem. Asian J.*, 2017, **12**, 1305-1308.
148. M. Sako, K. Higashida, G. T. Kamble, K. Kaut, A. Kumar, Y. Hirose, D.-Y. Zhou, T. Suzuki, M. Rueping, T. Maegawa, S. Takizawa and H. Sasai, *Org. Chem. Front.*, 2021, **8**, 4878-4885.
149. G. T. Kamble, M. S. H. Salem, T. Abe, H. Park, M. Sako, S. Takizawa and H. Sasai, *Chem. Lett.*, 2021, **50**, 1755-1757.
150. K. V. N. Esguerra, W. Xu and J.-P. Lumb, *Chem*, 2017, **2**, 533-549.
151. T. Heinrich, H. Böttcher, R. Gericke, G. D. Bartoszyk, S. Anzali, C. A. Seyfried, H. E. Greiner and C. Van Amsterdam, *J. Med. Chem.*, 2004, **47**, 4684-4692.
152. J. F. López-Giménez and J. González-Maeso, in *Behavioral Neurobiology of Psychedelic Drugs*, Springer Berlin Heidelberg, 2017, DOI: 10.1007/7854_2017_478, pp. 45-73.
153. S. P. Singleton, A. I. Luppi, R. L. Carhart-Harris, J. Cruzat, L. Roseman, D. J. Nutt, G. Deco, M. L. Kringelbach, E. A. Stamatakis and A. Kuceyeski, *Nat. Commun.*, 2022, **13**.
154. H. Ding, P. L. Deroy, C. Perreault, A. Larivée, A. Siddiqui, C. G. Caldwell, S. Harran and P. G. Harran, *Angew. Chem. Int. Ed.*, 2015, **54**, 4818-4822.
155. X. Zheng, Y. Li, M. Guan, L. Wang, S. Wei, Y. C. Li, C. Y. Chang and Z. Xu, *Angew. Chem. Int. Ed.*, 2022, **61**.
156. L. M. Blair and J. Sperry, *Chem. Commun.*, 2016, **52**, 800-802.
157. Z. Zhang, S. Ray, L. Imlay, L. T. Callaghan, H. Niederstrasser, P. L. Mallipeddi, B. A. Posner, D. M.

Wetzel, M. A. Phillips and M. W. Smith, *Chem. Sci.*, 2021, **12**, 10388-10394.
158. A. Sagadevan, V. P. Charpe, A. Ragupathi and K. C. Hwang, *J. Am. Chem. Soc.*, 2017, **139**, 2896-2899.
159. U. A. Kshirsagar, C. Regev, R. Parnes and D. Pappo, *Org. Lett.*, 2013, **15**, 3174-3177.
160. S. Quideau, D. Deffieux, C. Douat-Casassus and L. Pouységu, *Angew. Chem. Int. Ed.*, 2011, **50**, 586-621.
161. J. Zhao, J. Xiao, Y. Wang and Y. Peng, *Chinese J. Org. Chem.*, 2021, **41**, 2933.
162. E. Gaster, Y. Vainer, A. Regev, S. Narute, K. Sudheendran, A. Werbeloff, H. Shalit and D. Pappo, *Angew. Chem. Int. Ed.*, 2015, **54**, 4198-4202.
163. U. A. Kshirsagar, R. Parnes, H. Goldshtein, R. Ofir, R. Zarivach and D. Pappo, *Eur. J. Chem.*, 2013, **19**, 13575-13583.
164. S. Narute and D. Pappo, *Org. Lett.*, 2017, **19**, 2917-2920.
165. J. Yang, G. Qiu, J. Jiang, Y. Hu, S. Chen, S. Zhang and Y. Zhang, *Adv. Synth. Catal.*, 2017, **359**, 2184-2190.
166. R. Parnes, U. A. Kshirsagar, A. Werbeloff, C. Regev and D. Pappo, *Org. Lett.*, 2012, **14**, 3324-3327.
167. J. M. Edwards, M. Mangion, J. B. Anderson, M. Rapposch and G. Hite, *Tetrahedron Lett.*, 1979, 4453-4456.